Iron Carbonyl, Nitrosyl, and Nitro Complexes of a Tetrapodal Pentadentate Amine Ligand: Synthesis, Electronic Structure, and Nitrite Reductase-like Reactivity

Jesús Pitarch López,[a] Frank W. Heinemann,[a] Raju Prakash,[a] Bernd A. Hess,[b] Olivier Horner,[c] Claudine Jeandey,[c] Jean-Louis Oddou,[c] Jean-Marc Latour,[c] and Andreas Grohmann*[a]

Dedicated to Professor Anthony G. Wedd on the occasion of his 60th birthday

Abstract: The tetrapodal pentaamine 2,6-$C_5H_3N[CMe(CH_2NH_2)_2]_2$ ($py{N_4}$, **1**) forms a series of octahedral iron(II) complexes of general formula $[Fe(L)(\mathbf{1})]X_n$ with a variety of small-molecule ligands L at the sixth coordination site (L = X = Br, $n = 1$ (**2**); L = CO, X = Br, $n = 2$ (**3**); L = NO, X = Br, $n = 2$ (**4**); $L = NO^+$, X = Br, $n = 3$ (**5**); $L = NO_2^-$, X = Br, $n = 1$ (**6**)). The bromo complex, which is remarkably stable towards hydrolysis and oxidation, serves as the precursor for all other complexes, which may be obtained by ligand exchange, employing CO, NO, $NOBF_4$, and $NaNO_2$, respectively. All complexes have been fully characterised, including solid-state structures in most cases. Attempts to obtain single crystals of **6** produced the dinuclear complex $[Fe_2\{\mu_2\text{-}(\eta^1\text{-}N{:}\eta^1\text{-}O)\text{-}NO_2\}(\mathbf{1})_2]Br_2PF_6$ (**7**), whose bridging NO_2^- unit, which is unsupported by bracketing ligands, is without precedent in the coordination chemistry of iron. Compound **2** has a high-spin electronic configuration with four unpaired electrons ($S = 2$), while the carbonyl complex **3** is low-spin ($S = 0$), as are complexes **5**, **6** and **7** ($S = 0$ in all cases); the 19 valence electron nitrosyl complex **4** has $S = ½$. Complex **4** and its oxidation product, **5** ($\{Fe(NO)\}^7$ and $\{Fe(NO)\}^6$ in the Feltham–Enemark notation) may be interconverted by a one-electron redox process. Both complexes are also accessible from the mononuclear nitro complex **6**: Treatment with acid produces the 18 valence electron NO^+ complex **5**, whereas hydrolysis in the absence of added protons (in methanolic solution) gives the 19 valence electron $NO^{\cdot}$ complex **4**, with formal reduction of the NO_2^- ligand. This reactivity mimicks the function of certain heme-dependent nitrite reductases. Density functional calculations for complexes **3**, **4** and **5** provide a description of the electronic structures and are compatible with the formulation of iron(II) in all cases; this is derived from the careful analysis of the combined IR, ESR and Mössbauer spectroscopic data, as well as structural parameters.

Keywords: chelates · iron · nitrite reductase · N ligands

Introduction

Iron-nitrogen coordination chemistry in oxidation states II and III is dominated by mono- or multidentate *imines*, especially in the case of FeN_x cores, with $x = 4$, 5, 6. Such ligands have π* orbitals available for back-donation of electron density from the metal, thereby contributing to the overall stability of the complexes.[1–3] By contrast, *aliphatic amines* have pure σ-donor character, which causes the central metal to have high electron density. Iron complexes of such ligands are known, but they are numerous only in the case of *macrocyclic* ligands, such as triazacyclononane,[4, 5] cyclam[6, 7] or sarcophagine,[8] for which complex stability is owed largely to the "macrocyclic" or the "cryptate effect".[9] In the case of *open-chain aliphatic amines*, complexes of iron are extremely rare. The known compounds undergo ready hydrolysis and/or oxidation, yielding stable iron–imino species in some cases[10, 11] and ill-defined rust-like decomposition products in others.[12, 13] Similarly, while the hexaammine complex $[Fe(NH_3)_6]^{2+}$ is known, it is stable only under very special conditions.[14, 15]

Our recent work introduced a highly symmetrical open-chain pentaamine ligand with an NN_4 donor set, which

[a] Priv.-Doz. Dr. A. Grohmann, Lic. Quím. J. Pitarch López, Dr. F. W. Heinemann, Dr. R. Prakash
Institut für Anorganische Chemie
Universität Erlangen-Nürnberg
Egerlandstrasse 1, 91058 Erlangen (Germany)
Fax: (+49) 9131-8527-367
E-mail: grohmann@anorganik.chemie.uni-erlangen.de

[b] Prof. B. A. Hess
Institut für Physikalische und Theoretische Chemie
Universität Erlangen-Nürnberg
Egerlandstrasse 3, 91058 Erlangen (Germany)

[c] Dr. O. Horner, Dr. C. Jeandey, Dr. J.-L. Oddou, Dr. J.-M. Latour
Laboratoire de Physicochimie des Métaux en Biologie
FRE CEA/CNRS/UJF 2427
Département Réponse et Dynamique Cellulaires
CEA/Grenoble, 38054 Grenoble Cedex 9 (France)

  0947-6539/02/0824-5709 $ 20.00+.50/0

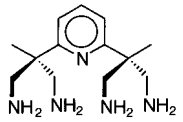

consists of a "central" pyridine unit and four equivalent aliphatic primary amino groups ("pyN$_4$", **1**). This polyamine has predominantly σ-donor character, is expected to render the coordinated metal ion electron-rich and imposes virtually no steric constraints; hence it may be construed as a "chelating analogue" of the pentaammine donor set $(NH_3)_5$. Initial reports detailed its coordination chemistry with Co^{III} and Ni^{II}.[16, 17] The ligand acts as a square-pyramidal "coordination cap", leaving a sixth coordination site for a small monodentate ligand in complexes of overall octahedral geometry. We are currently exploring derivatives of such complexes,[18, 19] with functional groups appended to the basal donor atoms of **1**, that will engage in secondary interactions with the monodentate ligand, so as to control its binding and reactivity. Depending on the choice of functional group, binding of the monodentate ligand may—when compared to the parent complex with nonderivatised pyN$_4$—become reversible.

In contrast to the reported lability of iron(II) complexes with open-chain aliphatic amine ligands, we have found that complexation with the pentaamine **1** is facile, and that these complexes possess remarkable stability with respect to hydrolysis and oxidation. Indeed, an alkaline aqueous solution is the preferred medium of preparation in some cases. We report here on the bromo complex [FeBr(**1**)]Br, and the carbonyl and nitro derivatives that have been obtained from it by ligand exchange ([Fe(CO)(**1**)]Br$_2$ and [Fe(NO$_2$)(**1**)]Br). The nitro complex shows reactivity reminiscent of the action of certain nitrite reductases,[20] in that it may be transformed into a pair of homologous 18 and 19 valence-electron iron–nitrosyl complexes ([Fe(NO)(**1**)]Br$_3$ and [Fe(NO)(**1**)]Br$_2$), upon reaction with H^+ and H_2O, respectively, in methanol. Attempts to characterise structurally the mononuclear nitro complex led to the isolation of a dinuclear complex with an unprecedented feature in the coordination chemistry of iron(II), namely, a bridging μ_2-(η^1-*N*: η^1-*O*)-NO$_2$ ligand, supported only by intramolecular interligand hydrogen bonding.

Results

[FeBr(1)]Br (2): A degassed aqueous solution of stoichiometric amounts of **1**·4HBr (the acid form of the ligand facilitates its handling and storage) and FeSO$_4$ hydrate, and a 20-fold excess of NaBr, when treated with aqueous NaOH, will, at pH 8 to 9, precipitate a yellow microcrystalline solid which is the Fe^{II} bromo complex [FeBr(**1**)]Br (**2**; isolated yield 57%; Scheme 1). NaBr is needed to "salt out" the complex, and a precipitate is not usually obtained in its absence. The ^{1}H NMR spectrum of the complex (at room temperature) shows paramagnetically broadened signals, and the effective magnetic moment is $\mu_{eff} = 5.23$ (RT, solid state). Compound **2** is moderately stable in the presence of air in water or methanol.[21] Oxidation (as judged by the observation of a colour change) is instantaneous only in the case of the ion-exchanged perchlorate salt, in which the sixth coordination site is most likely occupied by an aqua ligand.[22] In the cyclic voltammogram, compound **2** has a quasi-reversible one-electron redox wave at +0.17 V (Fe^{II}/Fe^{III}). The Mössbauer spectrum consists of a symmetrical doublet with an isomer shift of $\delta_{Fe} = 1.09(1)$ mm s^{-1} and a quadrupole splitting of $\Delta E_Q = 2.45(1)$ mm s^{-1} (Figure 1 and Table 1; the noise is due to the fact that a large part of the 14 keV Mössbauer radiation is absorbed by bromide ion from residual NaBr in the sample, see Experimental Section for details of sample preparation). The solid-state structure (at 200 K) shows the NN$_4$ ligand to be mononucleating and pentadentate (Figure 2),[16, 17] as expected. All Fe–N bonds are of similar length (Table 2), with an average of 2.169(6) Å, and the N-Fe-Br moiety is nearly linear, with an angle of 176.1(2)°.

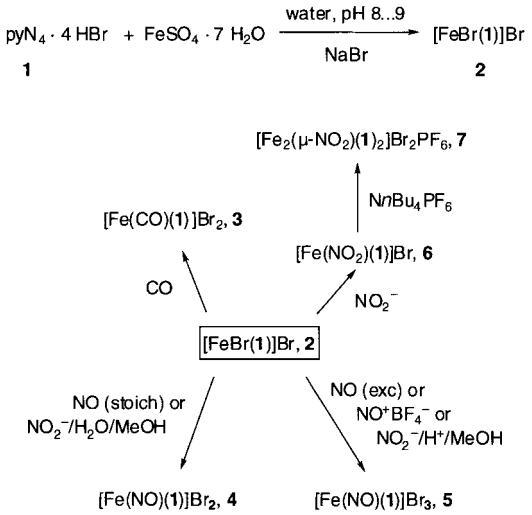

Scheme 1. Preparation of the pentaamine iron(II) bromo complex and its reactivity towards CO, NO, NO^+, and NO_2^-

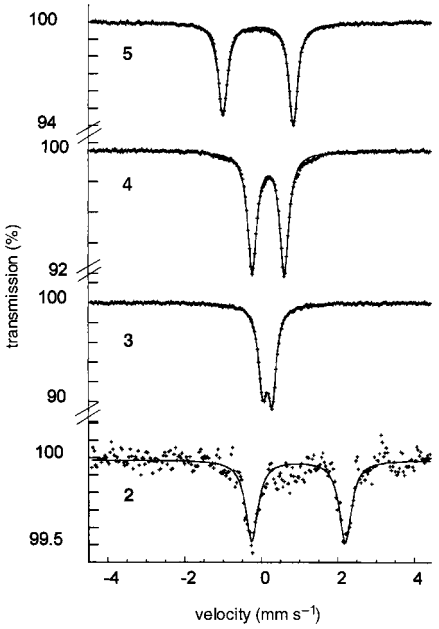

Figure 1. Zero-field Mössbauer spectra of solid complexes **2**, **3**, **4** and **5** at 77 K. The experimental spectra were fitted (solid curves) with the set of parameters listed in Table 1.

0947-6539/02/0824-5710 $ 20.00+.50/0 *Chem. Eur. J.* **2002**, *8*, No. 24

Table 1. Zero-field Mössbauer parameters[a] of solid complexes **2**, **3**, **4**, and **5**.

	[FeBr(**1**)]Br (**2**)	[Fe(CO)(**1**)](Br)$_2$ (**3**)	[Fe(NO)(**1**)](Br)$_2$ (**4**)	[Fe(NO)(**1**)](Br)$_3$ (**5**)
spin	2	0	½	0
δ_{Fe} [mm s^{-1}]	1.09(1)	0.29(1)	0.31(1)	0.04(1)
ΔE_Q [mm s^{-1}]	2.45(1)	0.25(1)	0.84(1)	1.84(1)
Γ_-[b] [mm s^{-1}]	0.39(3)	0.27(1)	0.29(1)	0.30(1)
Γ_+[b] [mm s^{-1}]	0.39(3)	0.25(1)	0.29(1)	0.27(1)

[a] Standard deviations are given in parentheses. [b] Γ = full width at half-maximum of the Lorentzian lines. Indices − and + refer to the lower and higher energy lines, respectively.

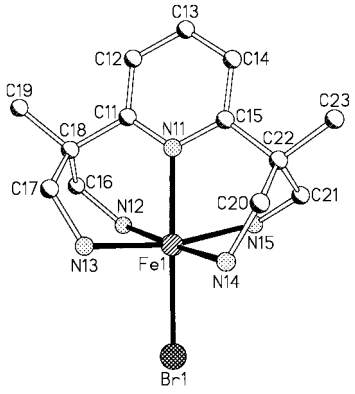

Figure 2. Molecular structure of the cation in **2**; for clarity, a ball-and-stick representation has been chosen, and hydrogen atoms have been omitted for clarity.

Table 2. Selected bond lengths [Å] and angles [°] for compounds **2**, **3**, **4** and **7** with estimated standard deviations in parentheses.

	2	**3**	**4**	**7**
Fe1–N11	2.197(6)	2.02(1)	2.095(5)	2.079(3)
Fe1–N12	2.165(6)	2.01(1)	2.004(6)	2.108(3)
Fe1–N13	2.140(6)	2.01(1)	2.023(5)	2.053(3)
Fe1–N14	2.171(6)	2.015(9)	2.010(5)	2.051(3)
Fe1–N15	2.174(6)	2.02(1)	2.030(6)	2.114(3)
Fe1–X[a]	2.673(2)	1.73(2)	1.737(6)	2.049(4)
X–O1[a]	–	1.20(2)	1.175(8)	–
N1–O1A	–	–	–	1.259(6)
N1–O2	–	–	–	1.118(6)
N11-Fe1-N12	86.4(2)	83.1(5)	82.9(2)	86.9(1)
N11-Fe1-N13	86.0(2)	89.6(4)	87.2(2)	91.6(1)
N11-Fe1-N14	90.1(2)	93.1(5)	91.5(2)	90.8(1)
N11-Fe1-N15	81.8(2)	87.4(4)	87.3(2)	86.5(1)
N12-Fe1-N13	83.1(2)	91.4(5)	91.9(2)	85.7(1)
N14-Fe1-N15	85.5(2)	84.5(4)	84.5(2)	86.1(1)
N13-Fe1-N14	94.8(2)	91.8(4)	92.0(2)	95.3(1)
N12-Fe1-N15	95.8(2)	92.1(4)	91.0(2)	93.0(1)
N11-Fe1-X[a]	176.1(2)	174.9(7)	172.5(3)	169.6(1)
N12-Fe1-N14	176.0(2)	174.9(5)	173.0(2)	177.5(1)
N13-Fe1-N15	167.8(2)	175.1(4)	173.4(2)	177.7(1)
Fe1-X-O1[a]	–	166(2)	139.4(5)	–
Fe1-N1-O1A	–	–	–	118.4(4)
Fe1-N1-O2	–	–	–	116.5(3)
O1A-N1-O2	–	–	–	125.1(6)
Fe1-N11-C11	119.1(5)	118.7(9)	119.0(4)	119.2(2)
Fe1-N12-C16	118.7(5)	116.7(8)	116.6(4)	116.5(2)
Fe1-N13-C17	115.7(5)	117.9(8)	118.4(4)	115.9(2)
N11-C11-C18	116.6(6)	118(1)	116.6(6)	117.1(3)
C11-C18-C16	110.9(6)	112(1)	110.9(6)	111.0(3)
C11-C18-C17	111.7(6)	109(1)	108.6(5)	110.6(3)
C18-C16-N12	114.2(6)	110(1)	112.6(6)	114.3(3)
C18-C17-N13	117.0(6)	113(1)	114.1(5)	114.6(3)

[a] **2**: X = Br1, **3**: X = C1, **4**: X = N1, **7**: X = N1; N1 is equivalent to O1A owing to disorder of the bridging nitro group, as shown in Figures 9 and 10.

[Fe(CO)(1)]Br$_2$ (3): Compound **2** reacts cleanly and in high yield with carbon monoxide in methanol, by displacement of the bromo ligand, to give the dicationic carbonyl complex. This precipitates from the solution at room temperature, and has been isolated as a yellow microcrystalline solid which is the dibromide salt, [Fe(CO)(**1**)]Br$_2$ (**3**; isolated yield 87%; Scheme 1). Solubility of complex **3**, while not in itself low, is increased considerably upon exchange of bromide for the BAr^F anion (BAr^F = [B(3,5-(CF$_3$)$_2$C$_6$H$_3$)$_4$]$^-$),[23] the resulting salt being readily soluble in methylene chloride.[24] The IR spectrum of solid **3** (KBr disc) has the CO stretching vibration at 1960 cm^{-1}. The compound is diamagnetic, with well-resolved ^{1}H and {^{1}H}^{13}C NMR spectra. They support a C_{2v} symmetrical structure of the cation in solution (see Experimental Section), and are overall similar to those observed for a series of cobalt(III) complexes of the pentaamine ligand.[16] The ^{13}C resonance of the carbonyl ligand occurs at δ = 220.71 ppm (D$_2$O). This is an extreme value for an Fe^{II}–CO complex when compared to the range of chemical shifts found for the CO adducts of hemoproteins and porphyrin-based model complexes (δ = 208 – 202 ppm).[25] Mössbauer spectroscopy yields δ_{Fe} = 0.29(1) mm s^{-1} for the isomer shift and ΔE_Q = 0.25(1) mm s^{-1} for the quadrupole splitting (Figure 1 and Table 1). In the solid-state structure (Figure 3), the mean

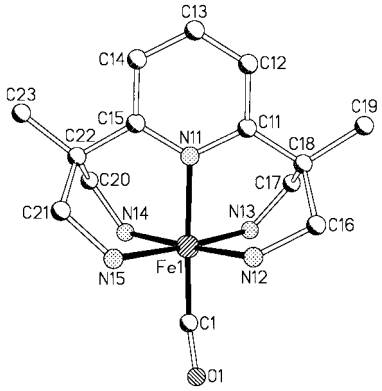

Figure 3. Molecular structure of the cation in **3**; hydrogen atoms have been omitted for clarity.

of the Fe–N bond lengths, which are all similar, is 2.02(1) Å. The coordination of the carbonyl ligand is essentially linear ($\sphericalangle$(Fe1-C1-O1) = 166(2)°), and the Fe–C bond length (1.73(2) Å) is similar to values determined for porphyrinato Fe^{II}–CO complexes with aromatic imines in the *trans* position (e.g., 1.744(5) Å[26]). Some of the primary amine nitrogen atoms have weak hydrogen-bonded contacts with the Br$^-$ counterions (e.g., d(N14-H14A ··· Br1) = 3.392(9) Å, $\sphericalangle$(NHBr) = 159(1)°; sum of van der Waals radii of N and Br: 3.4 Å[27]).

[Fe(NO)(1)]Br$_2$ (4): The reaction of the bromo complex **2** with a stoichiometric amount of nitrogen oxide, in methanol, gives an immediate colour change from orange to red, and eventually produces a reddish-brown precipitate that has been characterised as the 19 valence-electron iron – nitrosyl complex [Fe(NO)(**1**)]Br$_2$ (**4**), classified as {Fe(NO)}^{7} accord-

ing to the Feltham–Enemark notation (isolated yield 34%, Scheme 1).[28] Compound **4** is also formed by the reaction of a stoichiometric mixture of **1**·4HBr·MeOH, 4LiOMe, $FeCl_2$ and NO in methanol. It is characterised by an NO stretching frequency (KBr disc) of $\nu(NO) = 1620\ cm^{-1}$. The complex is paramagnetic, with an $S = ½$ ground state. Its predicted spin-only value of $1.73\ \mu_B$ lies within the range of magnetic moments measured at variable temperatures ($2-300$ K, $1.6 \leq \mu_{eff} \leq 2.0$; Figure 4). The EPR spectrum of **4**, which was

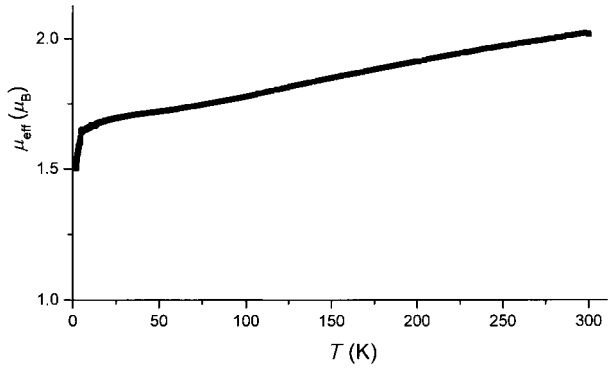

Figure 4. Temperature dependence of the magnetic moment μ_{eff} [μ_B] of a solid sample of **4**. At low temperatures, the magnetic moment decreases sharply due to intermolecular antiferromagnetic interactions.

obtained on the frozen sample at 115 K, is shown in Figure 5. The observed g tensor is rhombic ($g_1 = 2.051$, $g_2 = 2.005$, $g_3 = 1.966$), with ^{14}N hyperfine coupling due to the nitrosyl ligand resolved for g_2; the coupling constant is $A(^{14}NO) = 22.9$ G. The spectrum resembles that of the tetraphenylporphyrinatonitrosyliron complex with piperidine as an axial base ($g_1 = 2.080$, $g_2 = 2.040$, $g_3 = 2.003$; $A(^{14}NO) = 21.7$ G),[29] and a similar set of parameters was also determined for the nitrosyl derivative of myoglobin (MbNO).[30] Two redox waves are recorded in the cyclic voltammogram of **4** (Figure 6): a quasi-reversible one-electron oxidation ($E_{1/2} = +0.18$ V) and an irreversible reduction at -1.06 V. The oxidation yields the 18 valence electron complex **5** ({Fe(NO)}^{6}, below), whereas the reduction is assumed to produce a 20 valence electron species, {Fe(NO)}^{8}, for which there is precedent in the literature.[31, 32] The zero-field Mössbauer parameters (Figure 1 and Table 1) are $\delta_{Fe} = 0.31(1)\ mm\,s^{-1}$ and $\Delta E_Q = 0.84(1)\ mm\,s^{-1}$. The solid-state structure of this 19 valence

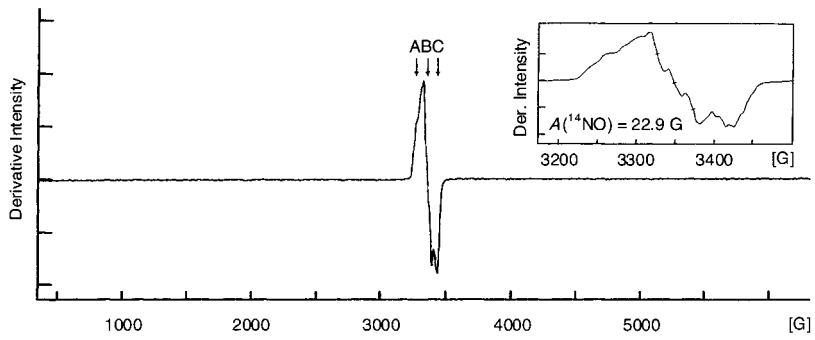

Figure 5. EPR spectrum of **4** at 130 K in DMF. Field markers A, B, C: $g = 2.051, 2.005, 1.966$. The enlargement of the feature at $g = 2.005$ (inset) shows superhyperfine structure due to ^{14}N coupling ($A(^{14}NO) = 22.9$ G).

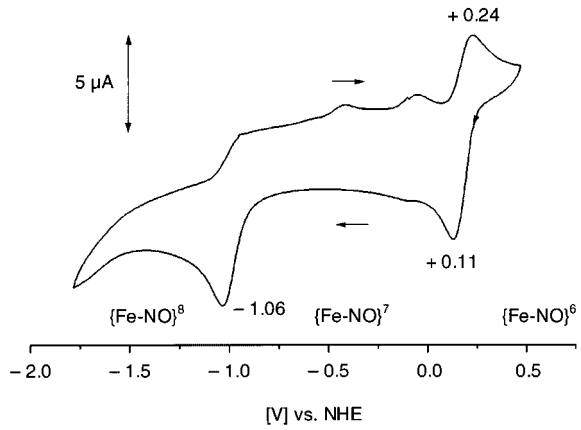

Figure 6. Cyclic voltammogram of **4** in DMF (for details see Experimental Section).

electron nitrosyl complex is presented in Figure 7, and relevant distances and angles are given in Table 2. Specifically, the equatorial Fe–N bond lengths are similar, with a mean of 2.017(6) Å, while the bond to the pyridine nitrogen atom, $Fe-N_{py}$, is 2.095(5) Å. The bond of the nitrosyl ligand to iron, d(Fe–NO), is 1.737(6) Å, and the ligand is coordinated at an angle of $\sphericalangle$(Fe1-N1-O1) = 139.4(5)°.

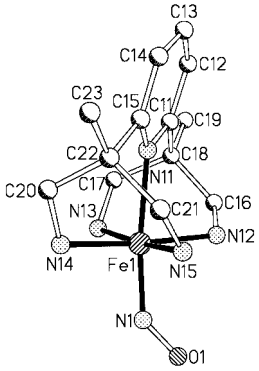

Figure 7. Molecular structure of the cation in **4**; hydrogen atoms have been omitted for clarity.

[Fe(NO)(1)]Br_3 (5): The 18 valence electron nitrosyl complex [Fe(NO)(**1**)]Br_3 (**5**, {Fe(NO)}^{6}), which is isoelectronic with the carbonyl complex **3**, is directly accessible from the bromo complex **2** by reaction with an NO^+ source such as $NOBF_4$ in a CH_2Cl_2 suspension. Alternatively, **5** has been obtained by prolonged reaction of **2** with NO gas in methanol, from which the product *precipitates* as a sparingly soluble yellow solid (when *dissolved* in methanol, **5** is unstable with respect to solvent-induced reduction to the 19 valence electron complex **4**, see below). Its formation by this route is presumably due to oxidation of the initially formed 19 valence electron complex **4** by small amounts of higher nitrogen oxides, such as NO_2 and N_2O_3, which are produced by reaction of NO with traces of oxygen in the gas stream.[33] Spectroscopic data also indicate spontaneous formation of **5** upon combination of the pentaamine ligand **1**, an iron(III) salt and NO in methanol. All samples are characterized by a strong absorption in the IR spectrum (KBr disc) at $1926\ cm^{-1}$ (ν(NO) stretch). Compound **5** is diamagnetic,

0947-6539/02/0824-5712 $ 20.00+.50/0 *Chem. Eur. J.* **2002**, *8*, No. 24

and its ^{1}H and ^{13}C NMR spectra show no unusual deviations from those of the carbonyl complex **3**. The cyclic voltammogram shows the same redox behaviour as the 19 valence electron complex **4**, as expected. The Mössbauer parameters (Figure 1 and Table 1) are entirely different from those of **4**, with values of $\delta_{Fe} = 0.04(1)$ mm s^{-1} and $\Delta E_Q = 1.84(1)$ mm s^{-1} for the isomer shift and quadrupole splitting, respectively. X-ray structural studies of **5** have so far been hampered by disorder in the anions, which has been difficult to resolve (the best crystals obtained so far are of a mixed bromide/sulfate salt, with Br^- and SO_4^{2-} sharing positions). It has, however, been possible to establish the connectivity and overall geometry of the cation, which is shown in Figure 8.

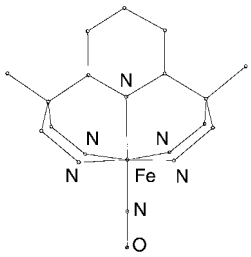

Figure 8. The overall connectivity and geometry of the cation in **5**, as obtained from a preliminary X-ray structure determination (see text).

[Fe(NO$_2$)(1)]Br (6) and its hydrolysis: Formation of the NO_2^- complex **6** upon addition of $NaNO_2$ to complex **2** in methanol is immediate, as judged by the colour change from orange to deep red and the deposition of an orange-red precipitate in 60 % isolated yield. The product has been fully characterised by IR, NMR and UV/Vis spectroscopy as well as other methods. Attempts to obtain single crystals of **6**, however, have invariably produced the nitrosyl complex {Fe(NO)}^{7} by slow hydrolysis, which has so far precluded structural characterisation of the mononuclear NO_2^- complex (cf. the description of the dinuclear iron nitro/nitrito complex, below). The IR spectrum of **6** (KBr disc) shows two very strong absorptions at 1258 and 1219 cm^{-1}, which are shifted to lower wavenumbers upon ^{15}N labelling (1245 and 1209 cm^{-1}, respectively), and which we assign to the symmetrical stretching vibration of an N-coordinated, nitro ligand. Nitrito ligands typically have their N–O stretching frequencies around 1450 and 1050 cm^{-1} ($\nu_{N=O}$, ν_{N-O}).[34] The nitro complex is diamagnetic with well-resolved NMR spectra, which, similar to the spectra of the carbonyl and {Fe(NO)}^{6} complexes, indicate a C_{2v} symmetrical cation in solution (see Experimental Section). In the FD mass spectrum, the molecular ion gives rise to the signal of highest intensity, and the cyclic voltammogram (DMSO solution) has one quasi-reversible one-electron redox wave at -0.07 V as the only feature, which we assign to the Fe^{II}/Fe^{III} couple of the mononuclear complex.

Addition of water to solutions of **6** (in sub-stoichiometric or stoichiometric amounts) in methanol under anaerobic conditions leads to the formation of the 19 valence electron complex [Fe(NO)(**1**)]Br$_2$ ({Fe(NO)}^{7}, **4**) as the major product (Scheme 1; IR spectroscopic evidence suggests that a small amount of the 18 valence electron complex **5** is also produced). Solutions set up to grow single crystals of **6** invariably produced single crystals of **4** unless moisture was rigorously excluded, in which case single crystals of the dinuclear complex **7** were obtained.

[Fe$_2${μ_2-(η^1-*N*:η^1-*O*)-NO$_2$}(1**)$_2$]Br$_2$PF$_6$ (7)**: Attempts to obtain single crystals of the mononuclear nitro complex **6** under strictly anhydrous conditions (redistilled solvents and freshly dried solids, see Experimental Section) gave a *dinuclear* iron(II) complex instead, containing an N,O-coordinated nitrite bridge (Scheme 1). SQUID measurements show the dinuclear complex to be diamagnetic over the full temperature range. The crystallisation was carried out in the presence of hexafluorophosphate, which may help to create a vacant coordination site on iron(II), in accord with previous observations of PF_6^--induced loss of a labile ligand from nickel(II).[17] The solid-state structure of the cation in **7** is shown in Figure 9. The Fe–N bond lengths to the pyridine and primary amine nitrogen atoms vary over the range 2.051(3) – 2.114(3) Å (see Table 2 for other relevant distances and angles). The NO_2 bridge shows disorder (which has been resolved), arising from the superposition of two possible orientations in the crystal structure in a 1:1 ratio (Figure 10). There is a crystallographic inversion centre at the midpoint of the N1–O1A bond vector, see Figure 9.

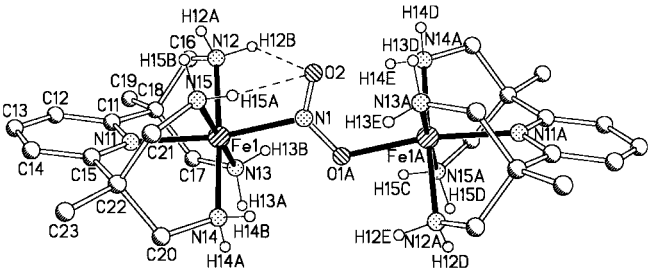

Figure 9. Molecular structure of the cation in **7**; intramolecular hydrogen bonds are shown as broken lines. The disorder of the bridging nitro/nitrito ligand is illustrated in Figure 10 (N1 ≡ O1; O1A ≡ N1A; O2A not shown).

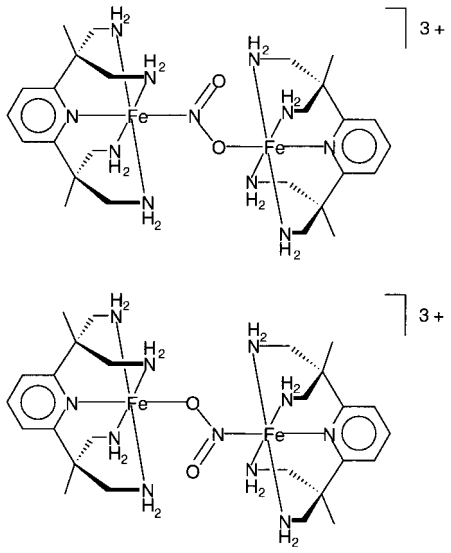

Figure 10. The two orientations of the cation of **7** in the solid state (occupancy factors: 0.5/0.5), which lead to the observed disorder. The underlying reason is a crystallographic inversion centre at the midpoint of the N1–O1A bond.

  0947-6539/02/0824-5713 $ 20.00+.50/0

Discussion

Reactivity: The hydrolysis reaction of **6**, in which the nitro ligand is reduced to coordinated nitric oxide, is remarkable in that it parallels the reactivity of certain heme cd_1-dependent nitrite reductases at physiological pH.[20] It is important to note that the hydrolysis of **6** to give **4** proceeds under neutral conditions. In acidic solution, uncoordinated NO_2^- is known to disproportionate into NO and NO_3^-. We therefore also investigated the reactivity of **6** in the presence of added protons (HBr or HBF_4), but found that these conditions lead to exclusive formation of the $\{Fe(NO)\}^6$ complex **5** (Scheme 1), which precipitates from solution. This reaction corresponds to the formal generation of NO^+ from NO_2^- and H^+ by loss of water, aided by metal coordination of the NO_2^- ligand; disproportionation is not observed. While this reaction is straightforward, it is more difficult to suggest a mechanism for the production of **4**. The reduction equivalents necessary for the $NO_2^- \rightarrow NO$ conversion may either be supplied by the pentaamine ligand[35] (which would explain the rather low yield of **4**) or by part of the Fe^{II} ions, which should lead to the formation of **4** (which contains formal Fe^{II}) and an Fe^{III} species in a 1:1 ratio. The Fe^{III} species could be the aqua complex $[Fe(OH_2)(\mathbf{1})]X_3$, but this has been found in separate work to produce the dinuclear oxo complex $[(\mathbf{1})Fe(\mu\text{-}O)Fe(\mathbf{1})]X_4$ by condensation,[36] and we have so far no indication for this product. However, partial formation of Fe^{III} has been shown to occur in the nitric-oxide-forming reaction between an iron(II) dithiocarbamate complex and nitrite.[37]

The most likely explanation for the observed reactivity, however, is to invoke methanol as a reducing agent. Addition of H^+ to a solution of **6** in methanol leads to the rapid formation of $\{Fe(NO)\}^6$ by loss of water from coordinated NO_2^-, and the product is protected against reduction by its low solubility. On addition of H_2O to a solution of **6** in methanol, the formation of $\{Fe(NO)\}^6$ proceeds much more slowly, so that whatever product is formed can immediately be reduced to $\{Fe(NO)\}^7$, with no precipitation of $\{Fe(NO)\}^6$. Methanol would thus play the same role in this functional model as do nonphysiological reducing agents (such as ascorbate) coupled with heme *c* in the case of heme cd_1-dependent nitrite reductase, for which such agents have been shown to sustain the function of the enzyme in vitro.[20, 38, 39] A comparison of these processes is given in Scheme 2. In our case, detection of the oxidised species deriving from methanol, a change of solvent and/or a kinetic study of the dependence of the reaction rate on the concentrations of nitrite and Fe^{II} are expected to resolve the question of which of the mechanisms outlined above applies.

Magnetism: The effective magnetic moment ($\mu_{eff} = 5.23$) determined for the bromo complex **2** indicates four unpaired electrons (calculated spin-only value for $S = 2$:4.90) and thus a high-spin Fe d^6 centre. Replacement of bromide by the strong-field ligand CO causes the carbonyl complex **3** to be low-spin, and, hence, diamagnetic. The nitrosyl complex $\{Fe(NO)\}^6$ is diamagnetic for similar reasons, whereas its reduction product, $\{Fe(NO)\}^7$, is paramagnetic due to the presence of one unpaired electron ($S = ½$). The diamagnetism of the nitro complex **6** is inferred from the appearance of the NMR spectra. The dinuclear nitro/nitrito-bridged iron complex **7** also shows diamagnetism (between 2 and 300 K), which suggests low-spin electronic configurations for the metal centres or, alternatively, strong antiferromagnetic coupling within the $\{Fe\text{-}NO_2\text{-}Fe\}$ core (which would have to be maintained over the full range of temperatures).

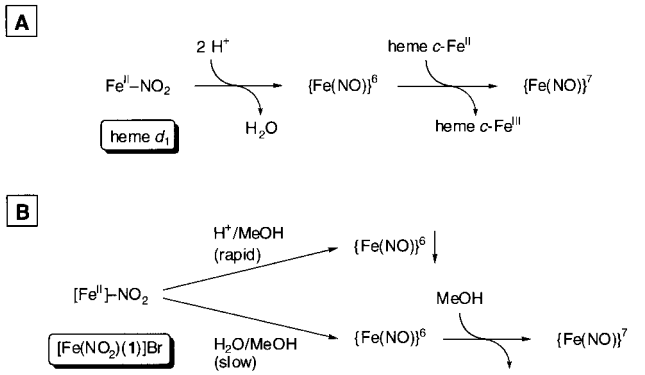

Scheme 2. Dehydration/reduction of nitrite by heme cd_1 nitrite reductase (A),[20, 38] and the reactivity of $[Fe(NO_2)(\mathbf{1})]Br$ described in this work (B).

Solid-state structures: The crystal structures presented here show the pentaamine ligand to be mononucleating throughout, with all five nitrogen donor atoms coordinated to the metal centre in approximate square pyramidal fashion. The distortion of the equatorial FeN_4 unit from planarity varies, but is moderate in all cases (cf. the angles N-Fe-N in Table 2). The mean Fe–N bond length in the bromo complex **2** (2.169(6) Å) is indicative of a high-spin Fe^{II} complex (cf. the value of 2.21(1) Å reported for $[Fe(en)_3]X_2$ (en = ethylenediamine)[40, 41]). Conditions that may induce a high-spin → low-spin transition in this complex have so far not been identified.[41]

The carbonyl complex **3** is unusual in that it appears to be the first octahedral Fe^{II}–CO complex with a non-porphyrin N donor environment to have been structurally characterised. Its most striking structural feature, when compared to **2**, is the sharp contraction of the Fe–N bonds, in accord with a low-spin Fe^{II} formulation. The mean bond length of 2.02(1) Å is in the range of values determined for low-spin Fe^{II} complexes of macrocyclic aliphatic amines[42] and podand polyamines with predominantly imine donor sets.[2, 41, 43] The other structural parameters, such as the bond angles at Fe, show no unusual deviation from their equivalents in the structure of **2** (Table 2), beyond what is to be expected for a central ion of smaller radius.

When comparing **3** with the 19 valence-electron nitrosyl complex **4**, the only striking difference involves the pyridine–iron bond lengths *trans* to the CO and NO ligands, respectively; these are $d(Fe\text{–}N) = 2.02(1)$ Å in **3**, and $d(Fe\text{–}N) = 2.095(5)$ Å in **4**. Whereas the bond lengths Fe–N_{NO} and N–O (1.737(6) Å and 1.175(8) Å, respectively) agree with previously reported structural data,[32, 44] the Fe-N-O angle in **4** (139.4(5)°) is 10–20° smaller than in other six-coordinate $\{Fe(NO)\}^7$ complexes,[32, 44] possibly due to an intramolecular

0947-6539/02/0824-5714 $ 20.00+.50/0 *Chem. Eur. J.* **2002**, *8*, No. 24

hydrogen bond between the nitrosyl ligand and one of the amine protons (N12–H12B···O1 2.926(8) Å, ∢(NHO) = 121°). By contrast, the Fe-N-O unit in the 18 valence electron complex **5** is linear, as shown by a preliminary structure determination. Approximate lengths of the Fe–N bonds between the iron ion and the pentadentate ligand are between 1.97 and 2.02 Å (and thus in accord with a low-spin formulation, cf. the carbonyl complex **3**), and the values for d(Fe–NO) and d(N–O) are 1.67 Å and 1.12 Å, respectively. The parameters involving the Fe-N-O unit are comparable to those of an 18 valence electron iron nitrosyl complex with an NS_4 ligand.[32]

While the bond angles in the {Fe(pyN_4)} fragment of the dinuclear complex **7** are similar to those of the other structures (Table 2), the Fe–N bonds to the pyridine and primary amine donor atoms are significantly longer (2.051(3) – 2.114(3) Å) than in the low-spin complexes **3** and **4**. This may reflect a high-spin configuration of the iron centres in **7**, which would have to be strongly antiferromagnetically coupled to give rise to the observed diamagnetism (cf. the section on magnetism). Further investigations are expected to clarify this point, and to delineate the role played by the N_6 and N_5O donor sets with respect to the iron centres in this mixed nitro/nitrito complex. The bond angles at the nitrogen atom of the NO_2 ligand deviate from the expected value of 120°, and the angle N_{py}-Fe-N_{NO2} is contracted to 169.6(1)° from the expected value of 180°. These distortions are, to a large part, due to intramolecular hydrogen bonds between the uncoordinated NO_2 oxygen atom and protons on the primary amino groups of the pentadentate ligand, as shown in Figure 9 (N12–H12B···O2 2.498 Å, ∢(NHO) = 108°; N15–H15A···O2 2.404 Å, ∢(NHO) = 113°). The μ_2-(η^1-*N*:η^1-*O*)-NO_2 bridge, which is unsupported by other ligands, is an unprecedented feature in the coordination chemistry of iron(II), and the only other instance in which this bonding mode has been found in a nonpolymeric compound appears to be a dinuclear copper(I) complex of macrocyclic ligands derived from triazacyclononane, synthesised as a model for the active sites of copper-dependent nitrite reductases.[45, 46]

Bonding description on the basis of spectroscopic (IR, ESR, Mössbauer) and structural data: The effective magnetic moments and the Fe–N bond lengths determined by X-ray crystallography indicate a high- and low-spin electronic configuration for iron(II) in the bromo complex **2** and the carbonyl complex **3**, respectively. The rather low frequency of the CO stretching vibration in the IR spectrum of solid **3** (KBr disc) at 1960 cm^{-1} points to a strong Fe–CO interaction,[47] as expected for the electron-rich NN_4 ligand environment.[48] Low values (1940 – 1960 cm^{-1}) were also reported for the rather unstable pentaamine iron(II) complexes [Fe(CO)(tetren)]X_2 (tetren = tetraethylenepentaamine; X = Cl, I, ClO_4).[13] Similarly, the low ν(NO) stretching frequency found for the 19 valence electron nitrosyl complex **4** (1620 cm^{-1}; KBr disc) points to an electron-rich metal centre, due to the almost exclusive σ-character of the NN_4 donor set, which enhances M → N–O back donation. By way of comparison, a low value has also been determined for *trans*-[FeCl(cyclam)(NO)]ClO_4 (1611 cm^{-1}).[31] The occurrence of ^{14}N-induced hyperfine splitting in the ESR spectrum of **4** shows that the singly occupied HOMO of the {Fe(NO)}^{7} unit retains a substantial amount of NO-based orbital character.[32, 49] The fact that the axial bond Fe–N_{py} in **4** is significantly elongated (2.095(5) Å) relative to the mean of the equatorial bonds (2.017(6) Å) suggests the HOMO in **4** to be antibonding with respect to Fe–N_{py} and bonding with respect to the Fe–N_{eq} interactions, a conclusion borne out by the molecular orbital calculations (below). Upon oxidation of **4** to the 18 valence electron complex **5** ({Fe(NO)}^{6}), the NO stretching frequency (KBr) shifts by more than 300 wavenumbers, to 1926 cm^{-1}. We interpret this drastic shift as a manifestation of the oxidation being largely centred on the NO ligand ($NO^{\cdot} \rightarrow NO^+$). Taken together, ESR and IR data provide a first indication that the nitrosyl complexes **4** and **5** contain $Fe^{II}/NO^{\cdot}$ and Fe^{II}/NO^+, respectively.

The assignment of formal iron oxidation states, especially in the case of the nitrosyl complexes, is surrounded by a good deal of controversy in the literature.[50, 51] We obtained the zero-field Mössbauer spectra of the mononuclear complexes **2**, **3**, **4** and **5** (as solids at 77 K) in order to correlate this series with other iron – amine complexes. The parameters determined for the bromo complex **2** (Table 1) are in accord with the description of the complex as a high-spin iron(II) (d^6) system,[52] and in excellent agreement with values obtained by Wieghardt et al. for a series of iron – cyclam complexes (cyclam = 1,4,8,11-tetraazacyclotetradecane), for which isomer shifts δ and assigned formal oxidation states were correlated.[31, 53] By contrast, no data are as yet available for carbonyl complexes of iron with non-porphyrin amine ligands, and **3** appears to be the first such complex to have been examined by Mössbauer spectroscopy. In comparison to **2**, both isomer shift δ_{Fe} and quadrupole splitting ΔE_Q are much smaller (Table 1). Usually, and particularly in the case of structurally related complexes, a lowered isomer shift correlates with an increase in oxidation state.[52] In the case of **3**, however, the assignment of a +II oxidation state is unequivocal, on the grounds of cation/anion balance in the solid-state structure and the notion that a description such as Fe^{III}/CO^- or Fe^{IV}/CO^{2-} has no parallel in iron – porphyrin chemistry. The observed trend for both Mössbauer parameters upon going from **2** to **3** may, however, be explained as follows: δ_{Fe} is expected to be reduced as the valence s-electron population increases, which it does as a consequence of reduced d-electron shielding due to the CO ligand being a strong π acid; ΔE_Q is smaller, since the asymmetry of the electron cloud around the nucleus is greatly reduced in a low-spin ($(t_{2g})^6$) as compared to a high-spin ($(t_{2g})^4(e_g)^2$) complex. It is noteworthy that the data for **3** do *not* fit Wieghardt's correlation of isomer shift and formal oxidation state for the series of iron – cyclam complexes mentioned above;[31] this would lead one to predict a value for **3** of $\delta_{Fe} \approx 0.53$ mm s^{-1} (low-spin Fe^{II}) or, conversely, a carbonyl complex with iron in a formal oxidation state of +III, and hence a CO^- ligand.

We now consider the data obtained for the nitrosyl complexes **4** and **5** ({Fe(NO)}^{7} and {Fe(NO)}^{6}), and begin with the 18 valence electron complex **5**. The very high IR stretching frequency at 1926 cm^{-1} (KBr) makes the formula-

  0947-6539/02/0824-5715 $ 20.00+.50/0

tion of an NO^+ ligand reasonable (in a localised bonding picture, electron density is removed from an *antibonding* orbital upon going from NO to NO^+, resulting in an increased force constant). Consequently, the metal ion in the diamagnetic complex **5** ($S=0$) must be in a low-spin iron(II) configuration, as in the case of the carbonyl complex **3**, whose CO stretching frequency is 1960 cm^{-1} (KBr). The Mössbauer parameters of **5**, however, are completely different (Table 1).[54] Based on the correlation proposed for iron–cyclam complexes,[31] the formal oxidation state of **5** predicted from its isomer shift would lie between +IV and +V. In our view, however, the measured parameters do not rule out the description of **5** as low-spin Fe^{II}/NO^+, since NO^+ is a much stronger π acid than even CO, thus decreasing the isomer shift considerably. Moreover, the increase of back-donation in **5** should induce some asymmetry in the electron distribution (which gives rise to a larger quadrupole splitting). Energy levels calculated for related compounds ($[Fe^{II}(CN)_5(CO)]^{3-}$ and $[Fe^{II}(CN)_5(NO)]^{2-}$) support this argument,[55] and are in accord with the qualitative (and by now classic) description of the bonding in metallonitrosyl complexes proposed by Enemark and Feltham.[56] The results presented here, particularly the evidence provided by the carbonyl complex **3**, suggest that the small-molecule ligands in **3** and **5** are best viewed as an isoelectronic set (i.e., CO and NO^+), so that the oxidation of the 19 valence electron nitrosyl complex **4**, which gives **5**, is ligand-centred. While conceding that the distinction is one of degrees and thus not entirely free from the blame of being academic (strong back-donation amounting to a formal intramolecular redox reaction), we rule out the description of **5** as being a combination of Fe^{IV} with an NO^- ligand, which has been proposed by Wieghardt et al. for an $\{Fe(NO)\}^6$ complex with a cyclam/chloride donor sphere.[31]

DFT calculations on $[Fe(CN)_5(NO)]^{2-}$ have provided an orbital diagram with a LUMO that is doubly degenerate and predominantly π^*_{NO} in character. One-electron reduction will give an NO-centred orbital as the new HOMO.[57] By way of analogy and short of a rigorous theoretical description of the bonding in **4** (which is given below), this situation would lead one to expect a rhombic *g* tensor with ^{14}NO hyperfine splitting for the ESR spectrum of **4**,[29] and this is what we observe. Moreover, if, as proposed, the reduction is ligand-centred, the value of the NO stretching frequency is expected to fall sharply (electron density is placed in a π^* NO orbital), as it does. We therefore describe our $\{Fe(NO)\}^7$ complex **4** ($S=½$) as a low-spin iron(II) species with a coordinated NO radical. Two other descriptions of the bonding situation are conceivable, namely, low-spin Fe^{III} coupled antiferromagnetically to NO^- (**A**), and intermediate spin Fe^{III} ($S=3/2$) also with antiferromagnetic coupling to NO^- (**B**). We rule out both for the following reasons: **A**: Comparison of the average equatorial iron–amine bond lengths in **4** (2.017(6) Å) and an authentic low-spin Fe^{III} complex of the pentaamine ligand ($[Fe(N_3)(\mathbf{1})]BrPF_6$, 1.998(3) Å)[58] shows the latter to have shorter bond lengths, in accord with its higher oxidation state. **B**: The isomer shifts of the carbonyl complex **3** and the $\{Fe(NO)\}^7$ complex **4** are very similar (Table 1), which means that the electron density at the nucleus is similar for both complexes, suggesting identical oxidation states. Moreover, the equatorial donor atoms impose no steric constraints, and the average equatorial iron–amine bond lengths are the same within experimental error (2.012(10) Å (**3**) and 2.017(6) Å (**4**)). To summarise, we suggest the following descriptions of the nitrosyl complexes presented here: $\{Fe(NO)\}^6$, **5**: low-spin iron(II)/NO^+; $\{Fe(NO)\}^7$, **4**: low-spin iron(II)/$NO^\bullet$. These views are in agreement with recent results published by Neese[59] for $\{Fe(NO)\}^7$ and $\{Fe(NO)\}^6$ species obtained with a cyclam–acetate ligand, and by Wieghardt et al.[60] for $\{FeNO\}^7$ and $\{FeNO\}^6$ species obtained with a pentadentate, pendent-arm macrocyclic ligand.

DFT calculations: We have carried out calculations in the framework of Kohn–Sham Density Functional Theory (DFT) for the complexes **3**, **4** and **5** in order to provide a description of the electronic structure of the molecules, and to compare this with the picture deduced from the experimental data, as outlined above. We used the program TURBOMOLE 5.4[61] for our all-electron DFT calculations and employed the BP86 functional[62, 63] with a triple-zeta valence-polarised Gaussian basis set[64] for the structure determination, making use of the Resolution of the Identity (RI) approximation.[65] All structures were fully optimised. A vibrational analysis confirming our stationary points as local minima on the potential surface was performed with the program SNF.[66] The harmonic stretching frequencies of the CO and NO ligands have been found at 2024, 1674, and 1939 cm^{-1} for **3**, **4**, and **5**, respectively (experimental values: 1960, 1620, and 1926 cm^{-1}, respectively). Bond lengths and angles are in good agreement with experimental values (Table 3). Since the X-ray structure analysis refers to the geometry of the molecule in the crystal structure, whereas the calculations describe a single molecule, a contribution of the crystal lattice (packing effect) is to be expected. Theoretical structure optimisations on $[Fe(CN)_5(NO)]^{2-}$ (ref. [67]) indicate that the bond lengths of the central atom to the first coordination shell are overstimated by an amount of the order of 0.02 Å in a single-molecule calculation, in agreement with our results, which yield values that are slightly too high, particularly for the bond lengths to the amine ligands. Whereas we find an essentially C_{2v} arrangement for the heavier atoms, the framework hydrogen atoms break the overall symmetry to C_1. This is due to the fact that a staggered conformation of the hydrogen atoms is energetically consid-

Table 3. Comparison of experimentally observed and calculated geometry parameters [bond lengths in Å, angles in °] for **3**, **4** and **5**.

	3 (theory)	**3** (exptl)	**4** (theory)	**4** (exptl)	**5** (theory)
Fe1–N11	2.03	2.02	2.08	2.10	2.02
Fe1–N12	2.04	2.01	2.07	2.00	2.08
Fe1–N13	2.05	2.01	2.05	2.02	2.05
Fe1–N14	2.03	2.02	2.04	2.01	2.08
Fe1–N15	2.06	2.02	2.04	2.03	2.05
Fe1–X	1.76	1.73	1.74	1.74	1.67
X–O1	1.16	1.20	1.19	1.18	1.15
N11-Fe1-X	179	175	177	173	180
Fe1-X-O1	179	166	139	139	179
C13-N11-Fe1	177	170	179	167	179

0947-6539/02/0824-5716 $ 20.00+.50/0 *Chem. Eur. J.* **2002**, *8*, No. 24

erably more favourable (by about 390 kJ mol^{-1}) than the all-eclipsed C_{2v} arrangement of the hydrogen atoms. While the calculations find that the local C_{2v} axis of the pyridine ring is collinear with the pseudotetragonal axis of the complex (leading to a C13-N11-Fe1 angle which is about 180°), the pyridine ring is tilted by more than 10° with respect to this axis in the X-ray structure. We find that the normal mode describing this movement is the lowest in all complexes (at about 55 cm^{-1}); hence, such a distortion should be facile if a small force is exerted on the complex due to the crystal environment.

Our minimum-energy structure for complex **4** is found to be stabilised by a hydrogen-bonding interaction to one of the amine hydrogen atoms, leading to an energy gain of the order of 10 kJ mol^{-1} as obtained by means of our recently developed method of estimating hydrogen-bond energies based on shared-electron numbers.[68] The calculated single-molecule minimum configuration of the NO unit has a dihedral angle to the plane of the pyridine ring slightly different from the experimental structure, and we used the calculated minimum for our further analysis. A calculation for a single molecule by using the coordinates taken from the X-ray structure is found higher in energy, but also exhibits a stabilisation of about 6 kJ mol^{-1} due to a hydrogen-bond interaction with one of the amine ligands.

To elucidate the electronic structure of species **3**, **4** and **5**, we have subjected the density obtained in our DFT calculation to several types of population analysis. In general, the assignment of charge to an atom within a polyatomic molecule cannot be carried out unambiguously, because it is at the heart of the concept of a covalent chemical bond that electrons are shared between atomic centres. Thus, for dividing those shared electrons up, a prescription not following directly from quantum mechanics is necessary; consequently, different population analyses will give different answers. Moreover, it is well known that the classical Mulliken population analysis[69, 70] in particular is strongly dependent on the basis set and doubtful for an extended basis set, as far as absolute values of charges are concerned. We try to avoid this dilemma by carrying out various types of analysis, and extracting only the common features. Thus, we are going to interpret the results of a Mulliken analysis, a natural bond orbital (NBO) analysis[71–73] and an analysis according to the Roby – Davidson – Ahlrichs protocol,[74] mainly for the purpose of describing the differences in electronic structure introduced upon reduction of **5** to **4**. Results of the three types of population analysis based on the calculated Kohn – Sham orbitals are given in Table 4 along with a charge analysis based on generalised atomic polar tensors,[75] which is dependent on the basis set only implicitly by way of the general quantum-mechanical description. From these analyses we can draw the following conclusions:

The oxidation state of iron (represented by its d occupation) does not change upon reduction of **5** to **4**. It is compatible with the formulation of Fe^{II} in each of the compounds **3**, **4** and **5**. Upon reduction, the charge on the NO fragment is appreciably reduced, which is compatible with a description of **5** as a nitrosyl (NO^+) compound, whereas the NO moiety in **4** is best described as neutral.

Table 4. Partial charges as calculated by various types of analysis of the density obtained in DFT.

	3 $[Fe(CO)(pyN_4)]^{2+}$	**5** $[Fe(NO)(pyN_4)]^{3+}$	**4** $[Fe(NO)(pyN_4)]^{2+}$ total $\alpha+\beta$	**4** spin polarisation $\alpha-\beta$
Mulliken population analysis				
charge on Fe	0.156	0.033	0.203	0.457
charge on X	0.031	0.239	0.045	0.320
charge on O	0.017	0.128	−0.052	0.197
charge on FeXO	0.204	0.400	0.197	0.974
charge on XO	0.048	0.367	−0.007	0.517
d-orbital occupation	6.55	6.60	6.64	0.45
Natural Bond Orbital analysis[71–73]				
charge on Fe		0.956	0.954	0.480
charge on X		0.171	−0.001	0.292
charge on O		0.028	−0.170	0.187
charge on FeXO		1.155	0.782	0.958
charge on XO		0.199	−0.171	0.479
d-orbital occupation		6.74	6.75	0.48
Roby – Davidson – Ahlrichs analysis[74]				
charge on Fe	0.381	0.599	0.537	0.434
charge on X	0.060	0.336	0.174	0.310
charge on O	0.041	0.138	−0.005	0.218
charge on FeXO	0.482	1.073	0.706	0.962
charge on XO	0.101	0.474	0.169	0.528
Charges from generalised atomic polar tensors[75]				
charge on Fe	−0.060	0.223	0.407	
charge on X	1.005	1.117	0.725	
charge on O	−0.695	−0.615	−0.641	
charge on FeXO	0.250	0.725	0.491	
charge on XO	0.310	0.502	0.084	

Whereas only part of the electron transferred upon reduction ends up on the FeNO fragment, practically all the spin polarisation is found on FeNO, about half of the magnetic moment being located on the iron d orbitals, the other half on NO. By contrast, practically all of the additional negative charge transferred to the FeNO fragment is located on NO, consistent with the finding that the singly occupied MO in **4** is practically exclusively of NO π* type (Mulliken population of the SOMO: 10 % Fe, 55 % N, 33 % O); see also Figures 11 and 12 for a visualisation of the SOMO and the total spin density of **4**. The explanation of the different behaviour of charge and magnetic moment is apparent from the NBO analysis, namely subtle differences in back-bonding interactions in **4** and **5**. The contribution of Fe orbitals acting as donors to NO π* orbitals can be found with significant contributions in second-order energy analysis in the case of **5** and the β-spin orbitals in **4**, whereas no such interactions are present in the α-spin orbital manifold of **4**. Thus, absence of back-donation in the latter case and even slightly increased back-donation in the β-spin orbital manifold (relative to **5**) results in appreciable net spin polarisation on the iron centre upon reduction, whereas still practically all of the charge transferred to FeNO ends up in the NO π* orbital.

The most prominent structural change upon reduction is the transition from a linear to a bent FeNO unit. This feature is, of course, well known from similar complexes and has occasionally been interpreted as a Jahn – Teller effect. The Jahn – Teller effect refers to the situation that upon unsymmetric occupation of a degenerate orbital in the central atom

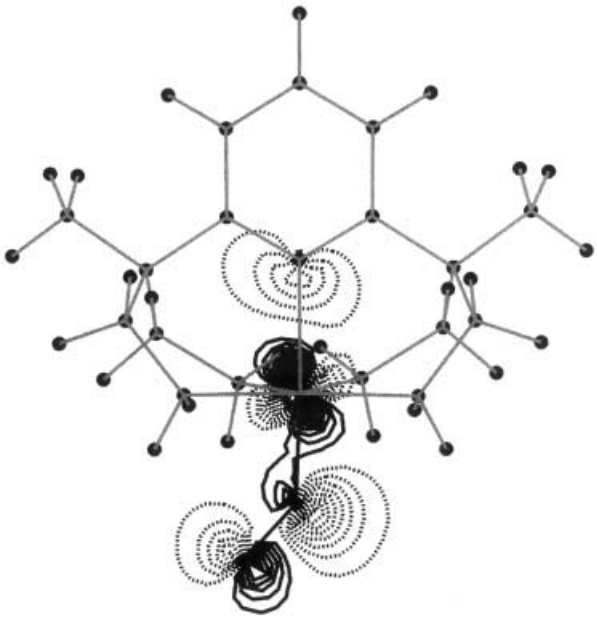

Figure 11. Contour plot of the singly occupied orbital (SOMO) of **4**.

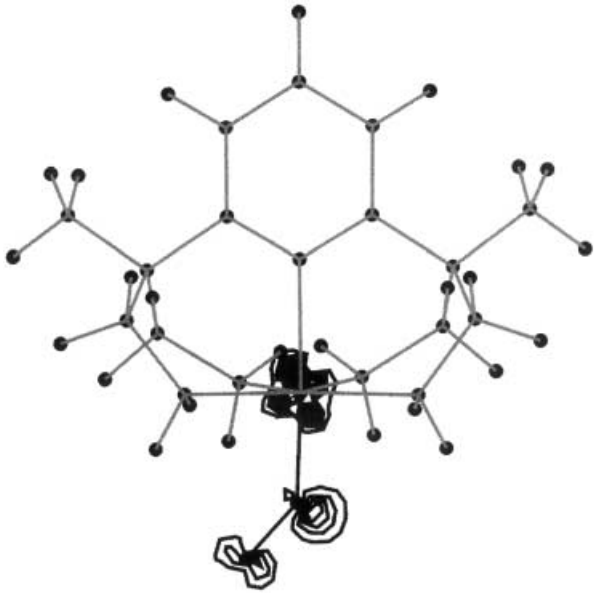

Figure 12. Contour plot of the spin density of **4**.

of a complex, a distortion of the complex takes place with a concomitant stabilisation of one of the degenerate molecular orbitals with respect to the others, which is then occupied by the additional electron.

From the discussion above it is clear that the additional electron is not located in an orbital of the iron atom, but rather in the π^* orbital of NO. This orbital is one of an (almost) degenerate pair of orbitals which occur as LUMOs of **5**. The analogue of the Jahn–Teller effect for this situation in the linear fragment FeNO is the Renner–Teller effect,[76, 77] which offers the possibility that one orbital out of the degenerate pair is stabilised upon bending of the linear moiety. It depends on the details of the electronic structure if such a stabilisation of one of the orbitals takes place, or rather one of the alternative cases that both or none of the two degenerate orbitals are stabilised. Thus, invoking the notion of a Renner–Teller effect to explain the observed bending is not particularly helpful, since the Renner–Teller effect generally allows for three possible responses of the system, including the one with a linear FeNO arrangement. Rather, we adopt the interpretation put forward by Guenzburger[57] that bending of the NO unit offers the possibility of an additional bonding interaction (of local σ symmetry) of NO with the metal, which cannot be present in a linear arrangement; this shows that stabilisation of *both* Renner–Teller orbitals is to be expected. This explains why several close-lying local minima have been observed for the geometrical arrangement of the NO ligand in similar cases,[57, 67] and indeed we have found two additional local minima with slightly different dihedral angles of the NO ligand with respect to the plane of the pyridine ring, having an energy less favourable than our optimised structure by 3.6 and 6.6 kJ mol^{-1}, respectively.

The SOMO is antibonding with respect to the pyridine ring and has very small contributions from the amine ligands. This explains the considerable increase of the bond length to the pyridine ring upon reduction of **5**. Notwithstanding this interpretation, the observed tetragonal distortion of the complex might also be interpreted as a Jahn–Teller-type distortion in the transition of **5** to **4**. This distortion has not been observed in a similar pair of a 18/19 valence electron complexes characterised by a sulfur-rich first-ligand sphere,[32] in which the sulfur orbitals effect a very closely spaced quasiband of orbitals near the Fermi surface; this acts as an electron buffer for electron redistribution at the iron centre and thus precludes appreciable energy gains upon distortion of the complex. The signature of this strong mixing of the sulfur orbitals is substantiated in the case of ref. [32] through a SOMO with appreciable antibonding contributions to *all* ligands.

Conclusion

This study describes an emerging rich coordination chemistry of the tetrapodal pentadentate amine ligand 2,6-$C_5H_3N[CMe(CH_2NH_2)_2]_2$ (pyN_4) towards iron(II). The complexes show remarkable stability, both with respect to oxidative degradation of the ligand and to unspecific hydrolysis. The ligand has predominant σ-donor character and thus provides an electron-rich coordination environment for the metal centre; this is conducive to unusual reactivity, such as the observed reduction of coordinated nitrite to NO. The assignment of formal iron oxidation states to the 18 and 19 valence electron nitrosyl complexes builds on the spectroscopic characteristics of the carbonyl complex, $[Fe(CO)(pyN_4)]Br_2$, which appears to be the first iron–CO complex with a non-porphyrin nitrogen-ligand environment to have been fully characterised. Experimental data and theoretical calculations are fully consistent, allowing the unambiguous formulation of the complexes presented here as containing iron(II) in all cases. Current work is concerned with modifications of the amine ligand that will make the coordination of NO reversible.

0947-6539/02/0824-5718 $ 20.00+.50/0 *Chem. Eur. J.* **2002**, *8*, No. 24

Experimental Section

Materials and instrumentation: Manipulations were performed under dinitrogen by using standard Schlenk techniques and freshly dried solvents. Reagents were AR grade or better and were purchased from Merck, Fluka, and Aldrich. **1**·4 HBr·MeOH and Na[B(3,5-$(CF_3)_2C_6H_3)_4$] (= $NaBAr^F$) were prepared as described previously.[24, 78] pH values were monitored with an NGOLD U455 pH meter (glass electrode). IR (KBr discs) and UV/Vis spectra (solvent: methanol) were recorded on Perkin – Elmer 16PC FTIR and Shimadzu UV-3101 PC instruments, respectively. NMR spectra were measured on a JEOL JNM-EX 270 spectrometer, and mass spectra were obtained on JEOL MSTATION 700 spectrometers. EPR spectra (Bruker ESP 300, spectrometer settings: X-band (9 GHz); power, 6.35 mW; modulation amplitude, 0.943 G; modulation frequency, 100 kHz; sweep time, 21 s; receiver gain, 10 000).

All Mössbauer measurements were performed on solid samples at 77 K, with a constant acceleration spectrometer calibrated with hematite. Isomer shifts are reported relative to an Fe metal standard at room temperature. The samples contain about 50 mg of solid complex in a nylon cell. The Mössbauer spectra were analysed by using home-made software. In addition, we also measured the Mössbauer spectra of all complexes (solid samples) between 4.2 and 200 K (data not shown), and no change in their electronic structure was detected in this temperature range.[60]

Room temperature magnetic moments were measured by using a Johnson – Matthey Gouy balance, with diamagnetic corrections calculated from Pascal's constants.[79] Variable temperature magnetic susceptibility measurements were carried out in the temperature range 2 – 300 K at a magnetic field of 0.1 T on polycrystalline samples using a magnetometer (Quantum Design MPMS-XL-5) equipped with a SQUID sensor. Diamagnetic corrections were applied by using Pascal's constants.[79] Cyclic voltammograms were recorded using an EG & G potentiostat PAR model 264A and a conventional three-electrode configuration consisting of a glassy carbon working electrode, a platinum auxiliary electrode and a Ag/AgCl reference electrode (room temperature; scan rate: 20 mV s^{-1}; supporting electrolyte: NBu_4PF_6 [10^{-1} M]; internal standard: ferrocene, $E(F_c/F_c^+) = +0.4$ V vs NHE[80]). The reversibility of the voltammograms and the number of electrons involved in the redox processes at 25 °C were determined as described in ref. [81]. Elemental analyses were performed on Carlo Erba Elemental Analysers 1106 and 1108.

X-ray crystallography: Crystal data for compounds **2**, **3**, **4**, and **7** are given in Table 5, and selected bond lengths and angles are listed in Table 2. Cation structures are presented in Figures 2, 3 and 7 – 9. All structures were solved by direct methods and refined by full-matrix least-squares procedures on F^2 using SHELXTL NT 5.10 (Bruker AXS, 1998). All non-hydrogen atoms were refined anisotropically. Treatment of hydrogen atoms: Compound **2**: All hydrogen atom positions were obtained from a difference Fourier synthesis, and both positional and common isotropic displacement parameters were kept constant during refinement. Compounds **3**, **4**: The hydrogen atoms were geometrically positioned and allowed to ride on their carrier atoms during refinement; their isotropic displacement parameters were tied to those of the adjacent C and N atoms by a factor of 1.5 (**3**; C, N), and 1.2 (**4**; C) or 1.5 (**4**; N). Compound **7**: All hydrogen atom positions were obtained from a difference Fourier synthesis; the positional parameters were refined, while a common isotropic displacement parameter was kept constant during refinement. Other remarks: Compound **2**: The compound crystallises with ⅓ of an MeOH molecule per formula unit. The solvate molecule is disordered around a threefold crystallographic rotation axis; its hydrogen atoms were omitted from the refinement. Compound **7**: The complex cation lies on a crystallographic inversion centre, which causes the bridging nitro ligand to be disordered (Figure 10). CCDC-189708 (**2**), CCDC-189709 (**3**), CCDC-189710 (**4**) and CCDC-189711 (**7**) contain the supplementary crystallographic data for this paper. These data can be obtained free of charge via www.ccdc.cam.ac.uk/conts/retrieving.html (or from the Cambridge Crystallographic Data Centre, 12 Union Road, Cambridge CB2 1EZ, UK; fax: (+44) 1223-336-033; or deposit@ccdc.cam.uk).

[FeBr(1)]Br (2): A solution of $FeSO_4 \cdot 7H_2O$ (0.56 g, 1.98 mmol) in water (3 mL), followed by solid NaBr (4.0 g, 39 mmol) was added to a solution of

Table 5. Crystallographic data for compounds **2**, **3**, **4** and **7**.

	2	**3**	**4**	**7**
formula	$C_{13}H_{25}Br_2FeN_5 \cdot \frac{1}{3}CH_3OH$	$C_{14}H_{25}Br_2FeN_5O$	$C_{13}H_{25}Br_2FeN_6O$	$C_{26}H_{50}Br_2F_6Fe_2N_{11}O_2P$
M_r	477.73	495.06	497.06	965.26
crystal system	rhombohedral	orthorhombic	orthorhombic	monoclinic
space group (no.)	$R\bar{3}c$ (no. 167)	$P2_12_12_1$ (no. 19)	$P2_12_12_1$ (no. 19)	$P2_1/c$ (no. 14)
a [Å]	21.825(3)	9.131(3)	9.194(1)	13.4024(2)
b [Å]	21.825(3)	10.308(4)	9.955(1)	10.7433(1)
c [Å]	40.270(5)	20.192(5)	20.042(2)	12.4809(2)
β [°]	90	90	90	95.874(1)
Z	36	4	4	4
V [Å^3]	16610(10)	1900(1)	1834.4(3)	1787.64(4)
ρ_{calcd} [g cm^{-3}]	1.719	1.730	1.800	1.793
diffractometer	Siemens P4	Nicolet R3m/V	Siemens P4	Nonius KappaCCD
λ[a] [Å]	0.71073	0.71073	0.71073	0.71073
crystal size [mm^3]	0.90 × 0.50 × 0.35	0.24 × 0.16 × 0.14	0.44 × 0.12 × 0.08	0.23 × 0.18 × 0.08
T [K]	200(2)	298(2)	200(2)	100(2)
absorption correction	Psi-scan	Psi-scan	Psi-scan	SORTAV
min/max transmission	0.0334/0.0858	0.0936/0.1204	0.054/0.083	0.418/0.579
scan	ω	ω	ω	ϕ,ω (2.0° and 24 s per frame)
2Θ range	$4 \le 2\Theta \le 54$	$4 \le 2\Theta \le 50$	$4 \le 2\Theta \le 54$	$7 \le 2\Theta \le 54$
measured reflections	8640	2539	4578	16795
unique reflections	4042	2381	3996	3879
observed reflections[b]	1812	1135	3184	3220
$\mu(Mo_{K\alpha})$ [mm^{-1}]	5.151	5.009	5.191	3.167
refined parameters	209	210	210	307
data/parameter ratio	19.3	11.3	19.0	12.6
$wR2$ (all data)[c]	0.1149	0.1108	0.1008	0.0868
$R1$ (obs. data)[d]	0.0593	0.0548	0.0481	0.0356
ρ_{fin} (max/min) [e Å^{-3}]	0.761/ – 0.477	0.596/ – 0.532	0.703/ – 0.479	0.895/ – 0.764
weighting scheme[e]	$k = 0.0351/l = 0$	$k = 0.0966/l = 3.7031$	$k = 0.0396/l = 2.2071$	$k = 0.0323/l = 5.2331$
abs. struct. parameter	–	0.01(3)	0.03(2)	–

[a] $Mo_{K\alpha}$, graphite monochromator. [b] With $F_o \ge 4\sigma(F)$. [c] $wR2 = (\{\Sigma[w(F_o^2 - F_c^2)^2]\}/\{\Sigma[w(F_o^2)^2]\})^{0.5}$. [d] $R1 = \Sigma||F_o| - |F_c||/\Sigma|F_o|$ for $F > 4\sigma(F)$. [e] $w = 1/[\sigma^2(F_o^2) + (kP)^2 + lP]$ and $P = (F_o^2 + 2F_c^2)/3$.

1·4HBr·MeOH (1.20 g, 1.98 mmol) in water (3 mL). Upon dissolution of the NaBr, the pH of the mixture was raised by dropwise addition of aqueous NaOH (6M) until a microcrystalline yellow precipitate started to form (pH 8–9). The solid was collected, and dried in vacuo (0.53 g, 57%). In some experiments, the material contained coprecipitated NaBr (0.7–2 equiv). Single crystals of the NaBr-free complex were obtained by isothermal diffusion of diethyl ether into a solution of the raw material in methanol. Elemental analysis calcd (%) for $C_{13}H_{25}Br_2FeN_5$ (467.0): C 33.42, H 5.36, N 15.00; found: C 33.17, H 5.62, N 14.41; IR (KBr): $\tilde{\nu}=3225$ (s), 3129 (s), 2915 (m), 1602 (m), 1583 (m), 1458 (m), 1097 (m), 1005 (s), 820 (m), 765 cm^{-1} (m); MS (FD): *m/z* (%): 386 (100), 388 (75) [M^+]; μ_{Eff} (spin only): 5.23 μ_B; cyclic voltammetry (RT, 10^{-3}M soln. in abs. MeCN): $E_{1/2}$ (Fe^{II}/Fe^{III}): +0.17 V, $\Delta E=125$ mV, $i_{pa}/i_{pc}=0.91$ (quasireversible, one electron); UV/Vis: λ_{max} (ε) = 403 nm (701 $dm^3mol^{-1}cm^{-1}$).

[Fe(CO)(1)]Br$_2$ (3): A stream of CO was passed through a solution of **2** (0.58 g, 1.24 mmol) in methanol (20 mL) for 30 min. Precipitation of the product set in immediately. The mixture was kept at −78 °C overnight and filtered at the same temperature. The product was collected as yellow microcrystals, which were dried in vacuo (0.49 g, 87%). Single crystals were obtained by isothermal diffusion of diethyl ether into a solution of **2** in methanol. Elemental analysis calcd (%) for $C_{14}H_{25}Br_2FeN_5O$ (495.0): C 33.96, H 5.09, N 14.15; found C 33.57, H 5.59, N 13.94; IR (KBr): $\tilde{\nu}=3175$ (s), 3122 (s), 2964 (m), 1960 (s) (CO), 1608 (m), 1597 (m), 1572 (w), 1465 (m), 1026 (m), 826 (w), 778 cm^{-1} (m); ^{1}H NMR ([D$_6$]DMSO, RT): $\delta=8.33$ (AB_2, 3 lines, ^3J(H,H) = 7.77/7.66 Hz, 1H; H^4), 7.88 (AB_2, 2 lines, ^3J(H,H) = 7.90 Hz, 2H; H^{3,5}), 3.51 (brs, 4H; −N*H*H), 2.36 (brs, 4H; −NH*H*), 2.11 (m, 8H; −CH_2−), 1.34 ppm (s, 6H; −CH_3); ^{1}H NMR (D_2O, RT): $\delta=8.20$ (AB_2, 3 lines, ^3J(H,H) = 7.90/8.14 Hz, 1H; H^4), 7.83 (AB_2, 2 lines, ^3J(H,H) = 8.14 Hz, 2H; H^{3,5}), 2.25 (d, ^2J(H,H) = 13.08 Hz, 4H; −C*H*H−), 2.13 (d, ^2J(H,H) = 12.84 Hz, 4H; −CH*H*−), 1.32 ppm (s, 6H; −CH_3); {^{1}H}^{13}C NMR (D_2O, RT): $\delta=220.71$ (s, CO), 166.79 (s, py-C2/6), 140.71 (s, py-C4), 121.24 (s, py-C3/5), 45.06 (s, −CH_2−), 43.48 (s, >C<), 21.52 ppm (s, −CH_3); ^{1}H NMR for [Fe(CO)(**1**)](BAr^F)$_2$ (CD_2Cl_2, RT): $\delta=8.42$ (AB_2, 3 lines, 1H; H^4), 8.01 (AB_2, 2 lines, 2H; H^{3,5}), 7.72 (s, 16H; BAr^F-H^{2,6}), 7.57 (s, 8H; BAr^F-H^4), 2.30 (brs, 4H; −N*H*H), 2.36 (s, 4H; −C*H*H−), 2.29 (s, 4H; −CH*H*−), 1.52 (s, 6H; −CH_3), 0.87 (s, 4H; −NH*H*); UV/Vis: λ_{max} (ε) = 317 (413), 402 nm (220 $dm^3mol^{-1}cm^{-1}$); Mass spectra (FD) do not show a peak for the parent ion; rather, intense signals at *m/z* (%) = 386/388 (100/80) suggest that [FeBr(**1**)]$^+$ is formed under these conditions. Cyclic voltammetry (RT, 10^{-3}M soln. in abs. DMSO): E_{pa}(Fe^{II}/Fe^{III}) = +0.79 V, $|E_{pa/2}-E_{pa}|=55$ mV (irreversible, one electron).

[Fe(NO)(1)]Br$_2$ (4, {Fe(NO)}^{7})

Method A: NO (14.4 mL, 0.60 mmol) was added by syringe to a solution of **2** (0.28 g, 0.60 mmol) in methanol (20 mL), and the mixture stirred vigorously. The colour of the solution changed from orange to red immediately, and a red precipitate appeared. Stirring was continued for 1 h, after which time the mixture was filtered to leave a red-brown solid which was washed with diethyl ether (5 mL) and dried in vacuo (0.10 g, 34%).

Method B: The compound was also prepared from a stoichiometric mixture of **1**·4HBr·MeOH, 4LiOMe, $FeCl_2$ and NO in methanol.

Method C: Single crystals of **4** were obtained as follows. NO (1 equiv, calculated for the bromo complex) was added by syringe to the aqueous mother liquor from a synthesis of the bromo complex **2** (above) with stirring, and the mixture kept at 4 °C overnight. Elemental analysis was satisfactory irrespective of the method of preparation.

Elemental analysis calcd (%) for $C_{13}H_{25}Br_2FeN_6O$ (497.0): C 31.41, H 5.07, N 16.91; found: C 31.60, H 5.28, N 16.65. IR (KBr): $\tilde{\nu}=3152$ (vs), 3084 (vs), 2962 (s), 2923 (s), 1620 (vs, NO), 1605 (s), 1593 (s), 1463 (m), 1395 (w), 1273 (w), 1209 (m), 1169 (w), 1039 (m), 1025 (m), 828 (w), 717 cm^{-1} (w); ESR (130 K, DMF glass): $g_1=2.050$, $g_2=2.005$, $g_3=1.966$; A(^{14}NO) = 22.9 G; Variable temperature magnetic susceptibility measurements: $S=1/2$, μ_{Eff} (2–300 K): 1.6–2.0 μ_B. UV/Vis: λ_{max} (ε) = 395 (560), 550 nm (112 $dm^3mol^{-1}cm^{-1}$); cyclic voltammetry (RT, 10^{-3}M soln. in abs. DMF): $E_{1/2}$ ({FeNO}^{7}/{FeNO}^{6}): + 0.18 V, $\Delta E=80$ mV, $i_{pa}/i_{pc}=0.98$ (quasi-reversible, one-electron), E_{pc} ({FeNO}^{7}/{FeNO}^{8}) = −1.06 V, $|E_{pc/2}-E_{pc}|=$ 50 mV (irreversible, one electron); MS (FD): see the comment for compound **3**, above.

[Fe(NO)(1)]Br$_3$ (5, {Fe(NO)}^{6})

Method A: A vigorous stream of NO was passed through a solution of **2** (0.22 g, 0.47 mmol) in methanol (15 mL). The colour of the solution changed from orange to deep red immediately, indicating the intermediate formation of the {Fe(NO)}^{7} complex (compound **4**, above). After about 10 min, a yellow precipitate started to form, and bubbling of NO was continued for 20 min. The solid was filtered off, washed with diethyl ether, and dried in vacuo (0.11 g, 41%).

Method B: [NO]$^+$[BF_4]$^-$ (30 mg, 1 equiv) as a solid in one portion was added to a suspension of **2** (0.12 g, 0.26 mmol) in methylene chloride (20 mL). Single crystals of **5** have so far proved difficult to obtain. Crystals used for a preliminary structure determination formed in an aqueous solution of the bromo complex **2**, with 1 equiv of $NaNO_2$ added, after about 1 week. There is, however, considerable disorder in the anions (see text). Elemental analysis calcd (%) for $C_{13}H_{25}Br_3FeN_6O$ (576.9): C 27.06, H 4.37, N 14.57; found: C 26.60, H 4.69, N 14.42; IR (KBr): $\tilde{\nu}=3196$ (vs), 3094 (vs), 3025 (vs), 2922 (s), 1926 (vs, NO), 1604 (m), 1576 (m), 1468 (m), 1223 (w), 1107 (w), 1032 (m), 823 (w), 717 (w), 478 cm^{-1} (w); UV/Vis: λ_{max} (ε) = 354 nm (1263 $dm^3mol^{-1}cm^{-1}$); ^{1}H NMR ([D$_6$]DMSO, RT): $\delta=8.55$ (AB_2, 3 lines, ^3J(HH) = 7.39/7.90 Hz, 1H; H^4), 8.04 (AB_2, 2 lines, ^3J(HH) = 7.90 Hz, 2H; H^{3,5}), 5.74 (brs, 4H; −N*H*H), 4.72 (brs, 4H; −NH*H*), 2.66 (m, 4H; −CH*H*−), 2.40 (m, 4H; −C*H*H−), 1.55 ppm (s, 6H; −CH_3); after addition of D_2O: $\delta=8.53$ (AB_2, 3 lines, ^3J(HH) = 7.77/7.90 Hz, 1H; H^4), 8.02 (AB_2, 2 lines, ^3J(HH) = 7.90 Hz, 2H; H^{3,5}), 2.64 (d, ^2J(HH) = 12.24 Hz, 4H; −CH*H*−), 2.36 (d, ^2J(HH) = 12.11 Hz, 4H; −C*H*H−), 1.53 ppm (s, 6H; −CH_3); {^{1}H}^{13}C NMR ([D$_6$]DMSO, RT): $\delta=161.9$ (s, py-C2/6), 143.6 (s, py-C4), 122.9 (s, py-C3/5), 46.6 (s, −CH_2−), 43.55 (s, >C<), 21.4 ppm (s, −CH_3); cyclic voltammetry: the same waves are observed as for **4** ({Fe(NO)}^{7}); MS (FD): see the comment for compound **3**, above.

[Fe(NO$_2$)(1)]Br (6): A solution of $NaNO_2$ (14.0 mg, 0.20 mmol) in methanol (2 mL) was added to an orange solution of [FeBr(**1**)]Br·2NaBr·H_2O (111 mg, 0.16 mmol) in methanol (8 mL). The colour changed to deep red immediately, and an orange-red precipitate appeared. The mixture was stirred at room temperature for 10 min, after which time the solid was collected by filtration, washed with Et_2O, and dried in vacuo overnight (56 mg, 60%). Elemental analysis calcd (%) for $C_{13}H_{25}BrFeN_6O_2\cdot CH_3OH$ (465.2): C 36.15, H 6.28, N 18.07; found: C 36.16, H 6.66, N 17.60; IR (KBr): $\tilde{\nu}=3280$ (vs), 3221 (vs), 2963 (s), 2927 (s), 2878 (s), 1607 (vs, NH scissor), 1577 (s), 1467 (s), 1395 (m), 1302 (m), 1258 (vs) (1245 $^{15}NO_2$), 1219 (vs) (1209 $^{15}NO_2$), 1161 (vs), 1099 (s), 1036 (vs), 818 (m), 764 (w), 620 (w), 450 cm^{-1} (w); ^{1}H NMR (CD_3OD, RT): $\delta=8.03$ (AB_2, 3 lines, ^3J(HH) = 7.90/7.79 Hz, 1H; H^4), 7.60 (AB_2, 2 lines, ^3J(HH) = 8.04 Hz, 2H; H^{3,5}), 2.55 (d, ^2J(HH) = 13.35 Hz, 4H; −C*H*H−), 2.23 (d, ^2J(HH) = 13.22 Hz, 4H; −CH*H*−), 1.34 ppm (s, 6H; −CH_3); {^{1}H}^{13}C NMR ([D$_6$]DMSO, RT): $\delta=171.5$ (s, py-C2/6), 137.1 (s, py-C4), 119.0 (s, py-C3/5), 46.7 (s, −CH_2−), 44.8 (s, >C<), 22.5 ppm (s, −CH_3); UV/Vis: λ_{max} (ε) = 472 nm (4009 $dm^3mol^{-1}cm^{-1}$); MS (FD): *m/z* (%): 355 (100) [M^++2H], 252 (80) [pyN_4], 386 (40) [FeBr(pyN_4)$^+$]; cyclic voltammetry (RT, 10^{-3}M soln. in abs. DMSO): $E_{1/2}$ (Fe^{II}/Fe^{III}): −0.07 V, $\Delta E=90$ mV, $i_{pa}/i_{pc}=0.97$ (quasireversible, one electron). From the filtrate of this preparation, after one week at 4 °C, were isolated single crystals of **4**, as identified by X-ray structure analysis. The formation of **4** is due to the presence of traces of water. Attempts to prepare and crystallise **6** with rigorous exlusion of moisture led to the isolation of the μ-NO_2-bridged dinuclear complex **7**.

[Fe$_2${μ_2-(η^1-*N*:η^1-*O*)-NO$_2$}(1**)$_2$]Br$_2$PF$_6$ (7)**: Solid LiOMe (87 mg, 2.29 mmol) was added to a suspension of **1**·4HBr·MeOH (0.35 g, 0.58 mmol) in methanol (6 mL); this produced a clear solution. After stirring for 10 min, the solvent was removed under reduced pressure, and the remaining colourless powder dried in vacuo overnight. This was then dissolved in methanol (redistilled from Na/NaOMe), and solid anhydrous [Fe(ac)$_2$] (101 mg, 0.58 mmol) was added, giving a dark orange solution. A solution of $NaNO_2$ (40 mg, 0.58 mmol; dried in an oil pump vacuum at room temperature for 2 d) in methanol (2 mL) was added, causing the colour of the mixture to change to a deep red immediately. The solution was filtered, and a small amount of an orange-red solid was collected (^{1}H NMR and IR data conform to [Fe(NO$_2$)(**1**)]Br, **6**, as obtained from [FeBr(**1**)]Br and $NaNO_2$). The filtrate and a 0.05M solution of N*n*Bu_4PF_6 in methanol were placed into the halves of a U-shaped glass tube separated by a glass frit. After 2 weeks, a small amount of single crystals had formed which were identified as **7** by X-ray crystallography. IR (KBr): $\tilde{\nu}=3377$ (s), 3353 (s), 3273 (vs), 3238 (vs), 3127 (s), 2963 (s), 2938 (s), 2881 (w), 1594 (s), 1578 (s),

0947-6539/02/0824-5720 $ 20.00+.50/0 *Chem. Eur. J.* **2002**, *8*, No. 24

1469 (s), 1397 (m), 1315 (m), 1260 (m), 1208 (m), 1163 (s, NO_2^-), 1085s, 1017 (s), 858 (vs, PF_6), 845 (vs) (PF_6), 810 (s), 752 (m), 557 cm^{-1} (s, PF_6); variable temperature magnetic susceptibility measurements (2 – 300 K) gave $S = 0$ over the full range of temperatures.

Reaction of [Fe(NO$_2$)(1)]Br (6) with H$^+$: Treatment of solutions of **6** in methanol with acid (HBr 48% or $HBF_4 \cdot Et_2O$, 2 equiv) yielded the 18 valence electron species $[Fe(NO)(\mathbf{1})]Br_3$ (**5**, $\{Fe(NO)\}^6$) as the only product, as identified by ^1H NMR and IR spectroscopy. Upon acidification of a suspension of $[Fe(^{15}NO_2)(\mathbf{1})]Br$ in methanol, the corresponding $\{Fe(^{15}NO)\}^6$ species had $\nu(^{15}NO)str = 1892\ cm^{-1}$, as opposed to $\nu(NO)str = 1926\ cm^{-1}$ for the unlabelled material (above).[82]

Acknowledgement

We thank Professor D. Sellmann for generous support of this work. Likewise, financial support from the Deutsche Forschungsgemeinschaft is gratefully acknowledged. J.P.L. is grateful for a European Union ERASMUS scholarship, which helped to initiate this project. We wish to thank Professor C. J. Gómez García (Universitat de València) for the variable temperature magnetic susceptibility measurements and Mr. Guido Marconi (Universität Erlangen-Nürnberg) for ESR measurements.

[1] P. V. Bernhardt, P. Comba, A. Mahu-Rickenbach, S. Stebler, S. Steiner, K. Várnagy, M. Zehnder, *Inorg. Chem.* **1992**, *31*, 4194 – 4200.
[2] M. E. de Vries, R. M. La Crois, G. Roelfes, H. Kooijman, A. L. Spek, R. Hage, B. L. Feringa, *J. Chem. Soc. Chem. Commun.* **1997**, 1549 – 1550.
[3] J. P. Collman, L. Fu, *Acc. Chem. Res.* **1999**, *32*, 455 – 463.
[4] L. Spiccia, G. D. Fallon, M. J. Grannas, P. J. Nichols, E. R. T. Tiekink, *Inorg. Chim. Acta* **1998**, *279*, 192 – 199.
[5] K. Meyer, E. Bill, B. Mienert, T. Weyhermüller, K. Wieghardt, *J. Am. Chem. Soc.* **1999**, *121*, 4859 – 4876.
[6] P. V. Bernhardt, T. Hambley, G. A. Lawrance, *J. Chem. Soc. Chem. Commun.* **1989**, 553 – 554.
[7] H. Börzel, P. Comba, H. Pritzkow, A. F. Sickmüller, *Inorg. Chem.* **1998**, *37*, 3853 – 3857.
[8] L. L. Martin, R. L. Martin, A. M. Sargeson, *Polyhedron* **1994**, *13*, 1969 – 1980.
[9] R. D. Hancock, A. E. Martell, *Comments Inorg. Chem.* **1988**, *6*, 237 – 284.
[10] V. L. Goedken, *J. Chem. Soc. Chem. Commun.* **1972**, 207 – 208.
[11] C.-Y. Liu, M.-C. Cheng, S.-M. Peng, S.-T. Liu, *Organometallics* **1994**, *13*, 4294 – 4299.
[12] N. Sadasivan, J. F. Endicott, *J. Am. Chem. Soc.* **1966**, *88*, 5468 – 5472.
[13] L. R. Melby, *Inorg. Chem.* **1970**, *9*, 2186 – 2188.
[14] G. W. Watt, W. A. Jenkins, *Inorg. Synth.* **1953**, *4*, 161 – 163.
[15] H. Behrens, *Adv. Organomet. Chem.* **1980**, *18*, 1 – 53.
[16] S. Schmidt, F. W. Heinemann, A. Grohmann, *Eur. J. Inorg. Chem.* **2000**, 1657 – 1667.
[17] C. Dietz, F. W. Heinemann, J. Kuhnigk, C. Krüger, M. Gerdan, A. X. Trautwein, A. Grohmann, *Eur. J. Inorg. Chem.* **1998**, 1041 – 1049.
[18] C. Dietz, F. W. Heinemann, A. Grohmann, *Eur. J. Inorg. Chem.* **1999**, 2147 – 2156.
[19] C. Zimmermann, F. W. Heinemann, A. Grohmann, *Eur. J. Inorg. Chem.* **2001**, 547 – 555.
[20] B. A. Averill, *Chem. Rev.* **1996**, *96*, 2951 – 2964.
[21] F. A. Deeney, C. J. Harding, G. G. Morgan, V. McKee, J. Nelson, S. J. Teat, W. Clegg, *J. Chem. Soc. Dalton Trans.* **1998**, 1837 – 1843.
[22] Preliminary results indicate the oxidation product to be the dinuclear iron(III) complex, $[Fe_2(\mu\text{-}O)(\mathbf{1})_2](ClO_4)_4$: J. Pitarch López, A. Grohmann, *Inorg. Chem. Commun.* **2002**, in press. Apparently, the Fe^{II}/Fe^{III} couple is sufficiently negative in this case, favouring the formation of a well-defined iron(III) complex over oxidative destruction of the amine ligand: see P. V. Bernhardt, T. Hambley, G. A. Lawrance, *J. Chem. Soc. Chem. Commun.* **1989**, 553 – 554.
[23] Anion exchange was carried out by adding a suspension of $Na[B(3,5\text{-}(CF_3)_2C_6H_3)_4]$ in CH_2Cl_2 to a stirred suspension of **3** in the same solvent, and removal of the the precipitated NaBr by filtration after about 30 min.
[24] M. Brookhart, B. Grant, A. F. Volpe, Jr., *Organometallics* **1992**, *11*, 3920 – 3922.
[25] M. Matsu-ura, F. Tani, Y. Naruta, *J. Am. Chem. Soc.* **2002**, *124*, 1941 – 1950.
[26] R. Salzmann, M. T. McMahon, N. Godbout, L. K. Sanders, M. Wojdelski, E. Oldfield, *J. Am. Chem. Soc.* **1999**, *121*, 3818 – 3828.
[27] A. Bondi, *J. Phys. Chem.* **1964**, *68*, 441 – 451.
[28] G. B. Richter-Addo, P. Legzdins, *Metal Nitrosyls*, Oxford University Press, Oxford, **1992**.
[29] B. B. Wayland, L. W. Olson, *J. Am. Chem. Soc.* **1974**, *96*, 6037 – 6041.
[30] L. C. Dickinson, J. C. W. Chien, *J. Am. Chem. Soc.* **1971**, *93*, 5036 – 5040.
[31] C. Hauser, T. Glaser, E. Bill, T. Weyhermüller, K. Wieghardt, *J. Am. Chem. Soc.* **2000**, *122*, 4352 – 4365.
[32] D. Sellmann, N. Blum, F. W. Heinemann, B. A. Hess, *Chem. Eur. J.* **2001**, *7*, 1874 – 1880.
[33] I. M. Lorković, P. C. Ford, *Inorg. Chem.* **2000**, *39*, 632 – 633.
[34] K. Nakamoto, *Infrared Spectra of Inorganic and Coordination Compounds*, 2nd ed., Wiley, New York, **1970**.
[35] The ligand pyN_4 has been shown to act as a reducing agent in the formation of a dinuclear cobalt(III) peroxo complex: S. Schmidt, F. W. Heinemann, A. Grohmann, *Eur. J. Inorg. Chem.* **2000**, 1657 – 1667.
[36] This complex has also been obtained by direct oxidation of $[Fe(H_2O)(pyN_4)]^{2+}$ with O_2, see ref. [22].
[37] K. Tsuchiya, M. Yoshizumi, H. Houchi, R. P. Mason, *J. Biol. Chem.* **2000**, *275*, 1551 – 1556.
[38] T. Kanti Das, E. K. Wilson, F. Cutruzzolà, M. Brunori, D. L. Rousseau, *Biochemistry* **2001**, *40*, 10774 – 10781.
[39] F. Cutruzzolà, K. Brown, E. K. Wilson, A. Bellelli, M. Arese, M. Tegoni, C. Cambillau, M. Brunori, *Proc. Natl. Acad. Sci. USA* **2001**, *98*, 2232 – 2237.
[40] J. Li, Z. Chen, T. J. Emge, D. M. Proserpio, *Inorg. Chem.* **1997**, *36*, 1437 – 1442.
[41] A. Diebold, K. S. Hagen, *Inorg. Chem.* **1998**, *37*, 215 – 223.
[42] J. C. A. Boeyens, A. G. S. Forbes, R. D. Hancock, K. Wieghardt, *Inorg. Chem.* **1985**, *24*, 2926 – 2931.
[43] A. H. R. Al-Obaidi, K. B. Jensen, J. J. McGarvey, H. Toftlund, B. Jensen, S. E. J. Bell, J. G. Carroll, *Inorg. Chem.* **1996**, *35*, 5055 – 5060.
[44] J. H. Enemark, R. D. Feltham, B. T. Huie, P. L. Johnson, K. Bizot Swedo, *J. Am. Chem. Soc.* **1977**, *99*, 3285 – 3292.
[45] J. A. Halfen, S. Mahapatra, M. M. Olmstead, W. B. Tolman, *J. Am. Chem. Soc.* **1994**, *116*, 2173 – 2174.
[46] J. A. Halfen, W. B. Tolman, *J. Am. Chem. Soc.* **1994**, *116*, 5475 – 5476.
[47] V. L. Goedken in *Coordination Chemistry of Macrocyclic Compounds* (Ed.: G. A. Melson), Plenum, New York, **1979**, Chapter 10.
[48] Pyridine is a weak π-acceptor: L. H. Gade, *Koordinationschemie*, Wiley-VCH, Weinheim **1998**, p. 108; D. A. House, J. Browning, L. Zipper, W. Marty, *Inorg. Chim. Acta* **1999**, *288*, 181 – 188.
[49] R. E. Shepherd, M. A. Sweetland, D. E. Junker, *J. Inorg. Biochem.* **1997**, *65*, 1 – 14.
[50] For an early example of conflicting assignments, see: H. Mosbæk, K. G. Poulsen, *J. Chem. Soc. Chem. Commun.* **1969**, 479 – 480; G. Rindorf, H. Mosbæk, K. G. Poulsen, *Acta Chem. Scand.* **1970**, *24*, 742 – 743.
[51] For a very recent example of reversible Fe^{III}/NO coordination, see: A. K. Patra, R. Afshar, M. M. Olmstead, P. K. Mascharak, *Angew. Chem.* **2002**, *114*, 2622 – 2625; *Angew. Chem. Int. Ed.* **2002**, *41*, 2512 – 2515.
[52] R. V. Parish in *NMR, NQR, EPR, and Mössbauer Spectroscopy in Inorganic Chemistry*, Ellis Horwood, Chichester, **1990**, p. 128.
[53] D. Marlin, P. Mascharak, *Chemtracts: Inorg. Chem.* **2000**, *13*, 539 – 546.
[54] Mössbauer spectral data for a recently reported $\{Fe(NO)\}^6$ complex with an $N_2S_3Fe(NO)$ core are very similar to those of **5**: C. A. Grapperhaus, A. K. Patra, M. S. Mashuta, *Inorg. Chem.* **2002**, *41*, 1039 – 1041.
[55] M. Braga, A. C. Pavão, J. R. Leite, *Phys. Rev. B* **1981**, *23*, 4328 – 4336.
[56] This bonding description is based on molecular orbital correlation diagrams that examine the nature of the highest-occupied molecular orbital in order to ascertain the structural consequences fo the M(NO) moiety: J. H. Enemark, R. D. Feltham, *Coord. Chem. Rev.* **1974**, *13*, 339 – 406.
[57] J. A. Gómez, D. Guenzburger, *Chem. Phys.* **2000**, *253*, 73 – 89.

  0947-6539/02/0824-5721 $ 20.00+.50/0

[58] J. Pitarch López, A. Grohmann, unpublished results.
[59] F. Neese, *EUROBIC-6, Book of Abstracts* **2002**, 282.
[60] M. Li, D. Bonnet, E. Bill, F. Neese, T. Weyhermüller, N. Blum, D. Sellmann, K. Wieghardt, *Inorg. Chem.* **2002**, *41*, 3444 – 3456.
[61] R. Ahlrichs, M. Bär, M. Häser, H. Horn, C. Kölmel, *Chem. Phys. Lett.* **1989**, *162*, 165 – 169.
[62] A. D. Becke, *Phys. Rev. A* **1988**, *38*, 3098 – 3100.
[63] J. P. Perdew, Y. Wang, *Phys. Rev. B* **1992**, *45*, 13244 – 13249.
[64] A. Schäfer, C. Huber, R. Ahlrichs, *J. Chem. Phys.* **1994**, *100*, 5829 – 5835.
[65] K. Eichkorn, F. Weigend, O. Treutler, R. Ahlrichs, *Theor. Chem. Acc.* **1997**, *97*, 119 – 124.
[66] J. Neugebauer, M. Reiher, C. Kind, B. A. Hess, *J. Comput. Chem.* **2002**, *23*, 895 – 910.
[67] B. Delley, J. Schefer, T. Woike, *J. Chem. Phys.* **1997**, *107*, 10067 – 10074.
[68] M. Reiher, D. Sellmann, B. A. Hess, *Theor. Chem. Acc.* **2001**, *106*, 379 – 392.
[69] R. S. Mulliken, *J. Chem. Phys.* **1955**, *23*, 1833 – 1841.
[70] R. S. Mulliken, *J. Chem. Phys.* **1955**, *23*, 1841 – 1849.
[71] J. P. Foster, F. Weinhold, *J. Am. Chem. Soc.* **1980**, *102*, 7211 – 7218.
[72] A. E. Reed, F. Weinhold, *J. Chem. Phys.* **1983**, *78*, 4066 – 4073.
[73] E. D. Glendening, J. K. Badenhoop, A. E. Reed, J. E. Carpenter, F. Weinhold, unpublished results.
[74] R. Heinzmann, R. Ahlrichs, *Theor. Chim. Acta* **1976**, *42*, 33 – 45.
[75] J. Cioslowski, *J. Am. Chem. Soc.* **1989**, *111*, 8333 – 8336.
[76] P. Jensen, G. Osmann, P. R. Bunker in *Computational Molecular Spectroscopy* (Eds.: P. Jensen, P. R. Bunker), Wiley, Chichester, **2000**, p. 485.
[77] J. M. Brown in *Computational Molecular Spectroscopy* (Eds.: P. Jensen, P. R. Bunker), Wiley, Chichester, **2000**, p. 518.
[78] S. Schmidt, L. Omnès, F. W. Heinemann, J. Kuhnigk, C. Krüger, A. Grohmann, *Z. Naturforsch. Teil B* **1998**, *53*, 946 – 954.
[79] O. Kahn, *Molecular Magnetism*, VCH, New York, **1993**.
[80] H.-M. Koepp, H. Wendt, H. Strehlow, *Z. Elektrochem.* **1960**, *64*, 483 – 491.
[81] A. J. Bard, L. R. Faulkner, *Electrochemical Methods, Fundamentals and Applications*, Wiley, New York, **1980**.
[82] S. J. George, J. W. A. Allen, S. J. Ferguson, R. N. F. Thorneley, *J. Biol. Chem.* **2000**, *275*, 33231 – 33237.

Received: July 18, 2002 [F4258]

  0947-6539/02/0824-5722 $ 20.00+.50/0